IEEE TRANSACTIONS ON WIRELESS COMMUNICATIONS, VOL. 16, NO. 11, NOVEMBER 2017

Energy Efficiency Evaluation of Multi-Tier Cellular Uplink Transmission Under Maximum Power Constraint

Jing Zhang, *Member, IEEE*, Lin Xiang, *Student Member, IEEE*, Derrick Wing Kwan Ng, *Member, IEEE*, Minho Jo, *Senior Member, IEEE*, and Min Chen, *Senior Member, IEEE*

Abstract—This paper evaluates the energy efficiency of uplink transmission in heterogeneous cellular networks (HetNets), where fractional power control (FPC) is applied at user equipments (UEs) subject to a maximum transmit power constraint. We first consider an arbitrary deterministic HetNet and characterize the properties of energy efficiency for UEs in different path loss regimes, or different access regions. By introducing the notion of transfer path loss, we reveal that, for UE whose path loss is below the transfer path loss, its energy efficiency highly depends on the value of power control coefficient adopted by FPC. In contrast, for UE with path loss above the transfer path loss, the uplink energy efficiency asymptotically decreases inversely with path loss, independent of the adopted power control coefficient. Based on these properties, we characterize the optimal power control coefficients for maximizing the energy efficiency of FPC in different access regions. Next, we extend the analysis to stochastic HetNets where UEs and BSs are distributed as independent Poisson point processes, and investigate the distribution of transmit power for uplink UEs. Moreover, the probability of truncation outage due to constrained maximal transmit power, as well as the average energy efficiency of UEs are analytically derived as functions of the BS and UE densities, power control

coefficient, and receiver threshold. Simulation results validate the analytical results, show the consistency between deterministic and stochastic analyses, and suggest suitable power control coefficient for achieving energy efficient uplink transmission by FPC in HetNets.

Index Terms—Wireless heterogeneous networks, power control, energy efficiency, uplink transmission.

I. INTRODUCTION

WITH the rapid development of wireless communication industry, the number of global mobile devices and connections has grown to 7.9 billion by 2015 and will be 11.6 billion in 2020 [1]. The large number of user devices have brought huge traffic demand and high energy consumption [2]. To support the traffic demand ecologically, energy efficiency analysis for wireless networks is crucial. In fact, energy efficiency of point-to-point wireless links has been well studied in the early literature. In particular, assuming an infinite blocklength of transmission codewords, the information theoretic analysis in [3] revealed that the energy efficiency of additive white Gaussian noise (AWGN) channel decreases monotonically with the channel capacity. However, the analysis in [3] optimistically ignored the circuit power consumption. In practice, when circuit power consumption is taken into account, signal transmission over a long duration may no longer be energy efficient since the total power consumption will increase with the blocklength [4].

Different from point-to-point wireless links, energy efficiency analysis for wireless networks is complicated due to the presence of co-channel interference and the need to meet network coverage requirements. Moreover, the spatial and temporal variations of the traffic demands from user equipments (UEs) are difficult to be identified [5]. In [6], the energy efficiency for wireless networks employing advanced transmission techniques including orthogonal frequency division multiple access (OFDMA), multiple-input multiple-output (MIMO), and relay transmission, was investigated. In [7], the authors identified four key trade-offs between energy efficiency and other network performance metrics including deployment efficiency, spectrum efficiency, bandwidth, and delay. Considering downlink multiuser orthogonal frequency division multiplexing in distributed antenna systems (OFDM-DAS), an energy-efficient resource (e.g., antenna, subcarrier, and transmit power) allocation scheme was proposed in [8], which

Manuscript received January 17, 2017; revised June 15, 2017; accepted August 3, 2017. Date of publication August 18, 2017; date of current version November 9, 2017. This work was supported in part by the Ministry of Science and Technology of China under Grant 2016YFE0119000, in part by the Korea–China Joint Research Center Program through National Research Foundation under Grant 2016K1A3A1A20006024, in part by the Korean Government, in part by the National Natural Science Foundation of China (NSFC) under Grant 61271224, Grant 61572380, and Grant 61572220, and in part by the NFSC Major International Joint Research Project under Grant 61210002. The work of D. W. K. Ng was supported by the Australian Research Council's Discovery Early Career Researcher Award Funding Scheme under Grant DE170100137. The associate editor coordinating the review of this paper and approving it for publication was G. C. Alexandropoulos. *(Corresponding author: Minho Jo.)*

J. Zhang is with the School of Electronic Information and Communications, Huazhong University of Science and Technology, Wuhan 430074, China (e-mail: zhangjing@hust.edu.cn).

L. Xiang is with the Institute for Digital Communications, Friedrich-Alexander University of Erlangen-Nuremberg, Erlangen 91058, Germany (e-mail: lin.xiang@fau.de).

D. W. K. Ng is with the School of Electrical Engineering and Telecommunications, University of New South Wales, Sydney, NSW 2052, Australia (e-mail: w.k.ng@unsw.edu.au).

M. Jo is with the Department of Computer Convergence Software, Korea University, Sejong Metropolitan City 30019, South Korea (e-mail: minhojo@korea.ac.kr).

M. Chen is with the Wuhan National Laboratory for Optoelectronics (WNLO) and the School of Computer Science and Technology, Huazhong University of Science and Technology, Wuhan 430074, China (e-mail: minchen@ieee.org).

Color versions of one or more of the figures in this paper are available online at http://ieeexplore.ieee.org.

Digital Object Identifier 10.1109/TWC.2017.2739142

1536-1276 © 2017 IEEE. Personal use is permitted, but republication/redistribution requires IEEE permission.
See http://www.ieee.org/publications_standards/publications/rights/index.html for more information.

solves the resource allocation optimization problem based on fractional programming techniques. Moreover, joint transmitter and receiver optimization was proposed for maximization of energy efficiency in OFDMA systems in [9]. Meanwhile, energy efficiency analysis has been extended from single-tier (homogeneous) cellular networks [6]–[9] to heterogeneous cellular networks (HetNets) [10]–[12]. It was shown in [10] that the energy efficiency of HetNets increases monotonically with the deployment density of small cells. The energy efficiency of HetNets by adopting energy harvesting small cell base stations (BSs) and traffic load adaptation in different tiers of HetNets was analyzed in [11]. Moreover, a low complexity macrocell user selection method for spectrum-power trading in multi-tier network was proposed in [12] to increase the trading energy efficiency of the macrocell users. However, the aforementioned works [5]–[12] usually assumed a deterministic cellular topology, which prevents close-form characterization for energy efficiency; hence, it is difficult to extend their results to large scale HetNets.

In this paper, we focus on analyzing the energy efficiency of large scale HetNets in the uplink. Improving the energy efficiency of uplink transmission is crucial for reducing the energy consumption network-wide and extending the operation hours of UEs, which usually have limited battery storage. For this purpose, uplink power control, e.g. via fractional power control (FPC), is a well-known effective approach. Recently, FPC has been adopted in 3GPP LTE-Advanced standard to conserve energy at UEs and mitigate interference in the network [13]. By FPC, the signal transmit power of UE is adjusted using a network-wide power control coefficient to meet the target signal-to-interference-and-noise ratio (SINR) requirement while avoiding excess interference to other UEs. However, as the transmission rate and the power consumption, both dependent on the power control coefficient of FPC, become coupled, energy efficiency analysis of FPC in the uplink is complicated. The majority of the literature only resort to Monte Carlo simulations to study FPC, which are usually time consuming, especially for large scale HetNets [14]–[17]. Moreover, when the maximal transmit power constraint is considered due to the linearity requirement of power amplifier as well as the battery storage limitation, the energy efficiency of FPC will depend on the power control coefficient and the receiver threshold jointly. In this case, choosing a suitable power control coefficient is nontrivial. To our knowledge, how to adjust the power control coefficient within constrained maximal transmit power for maximizing the energy efficiency of large scale HetNets has been rarely investigated.

Recently, stochastic geometry method has been applied to investigate the performance of large scale multi-tier HetNets [18]. By modeling the cellular network topology as a random point process, e.g. the Poisson point process (PPP), statistics of system performance can be easily obtained in closed form, without resorting to the time-consuming Monte Carlo simulations. In particular, the PPP model has been shown to be sufficiently accurate for modeling actual urban cellular networks [19], [20]. For this reason, the PPP model has been successfully applied for studying the downlink of large scale HetNets [21]. However, direct extension of the PPP model for analyzing FPC in the uplink is infeasible since, different from the downlink, the spatial distribution of interferers, i.e. interfering UEs, does not follow the PPP. This is because, by FPC, the interference power caused by the interfering UEs becomes correlated with their path losses to the desired BS. Besides, when orthogonal multiple access schemes, e.g., OFDMA, are adopted in the uplink, each cell allows only one user to operate on the typical resource block, which further enables a soft repulsion on the spatial distribution of the co-channel interferers. For these reasons, analytical results for performance analysis in the uplink are rarely obtained. Although various generative models [23], [24] have been proposed to approximate the spatial distribution of interferers in OFDMA Poisson cellular networks, they only apply in special cases such as single-tier (macro-only) networks [23] or channel-inversion based power control [24]. On the other hand, there has also been growing interest in studying various techniques such as offloading [25], spectrum sharing [26], fractional frequency reuse [27], and multi-stream carrier aggregation (MSCA) [28] for leveraging better trade-offs between spectral and energy efficiencies in multi-tier HetNets. However, joint consideration of these techniques and FPC for large scale HetNets is rare due to the aforementioned difficulties for analysis.

To address the above issues in this paper, we propose a framework for modeling and optimizing the energy efficiency of FPC in the uplink of large scale stochastic geometry HetNets, where UEs have constrained maximal transmit power. We evaluate the energy efficiency in both deterministic and stochastic cell topologies for qualitative and quantitative characterization purposes, respectively. First, for deterministic cell topology, or for a realization of the stochastic geometry HetNet where locations of BSs and UEs are fixed, we study the correlation between uplink energy efficiency and power control coefficient for UEs locating in different path loss regimes, i.e., different access regions. Based on the analytical results, we further characterize the optimal power control coefficient for maximization of the energy efficiency in different access regions. Next, taking into account the spatial distributions of BSs and UEs in stochastic geometry HetNets, we extend the deterministic analysis to evaluate the average energy efficiency of UEs. To address the difficulties in modeling the interferer locations, the interferer's propagation process is defined for modeling the path loss distribution of interfering UEs. We show that although the interferer's propagation process follows the Poisson-Voronoi perturbed lattice, it converges to an inhomogeneous PPP when a sufficiently strong log-normal shadowing effect is present. The convergence result is inspired by [29] and [30], where similar techniques have been applied to model the coverage and achievable rate in the uplink [29] as well as to study orthogonal multiple access [30]. However, different from [29] and [30], the distribution of transmission power and the truncation outage probability have to be newly derived in this paper for characterizing the average energy efficiency. Moreover, the deterministic analysis and optimization of FPC for fixed UEs and BSs is neither considered in [29] nor in [30].

The main contributions of this paper are summarized as follows:

1) We propose a comprehensive framework for modeling and optimizing the energy efficiency of FPC under maximal transmit power constraint. For given locations of BSs and UEs, we reveal that there exists a transfer path loss, which splits the cell into two access regions. The uplink energy efficiency of UE shows different properties in these access regions. We also derive the upper and lower bounds for the transfer path loss. Moreover, we investigate the optimal power control coefficient for maximizing the uplink energy efficiency of UE in different access regions. The bounds of path loss for different values of optimal power control coefficients are provided.

2) For randomly located BSs and UEs, we derive the average energy efficiency under FPC, which is based on characterizing the probability distribution of UE transmission power and the probability of UE in outage subject to the maximal transmit power constraint.

3) The analytical derivations are verified via Monte Carlo simulation results. Both the analytical and simulation results suggest that the maximal average energy efficiency is achieved when the receiver threshold is close, but not equal, to the maximal transmit power and the power control coefficient is adjusted accordingly.

The rest of this paper is organized as follows. In Section II, the system model of uplink power control scheme under maximal transmit power constraint in HetNets is presented. The transfer path loss for energy efficiency of UE and the bounds of transfer path loss for deterministic HetNets are described in Section III. Detailed properties for energy efficiency in different region are also revealed in this section. In Section IV, the distribution of transmit power, the truncation outage probability, and the average energy efficiency of UEs for stochastic HetNets are characterized. The derived results are validated in Section V by simulation results, where the impact of various system parameters on the uplink energy efficiency is illustrated. Finally, Section VI concludes the paper.

II. SYSTEM MODEL

As shown in Fig. 1, a K-tier HetNet system is deployed to provide seamless access service over the whole $\mathbb{R}^2$ plane. Let $m_i^{(k)}$ denote the location of BS i in tier $k \in \{1, 2, \cdots, K\}$. The location of BSs in tier k is denoted by $\Phi_k = \{m_i^{(k)}; i = 1, 2, 3 \cdots\}$, where the pilot transmit power of BSs in tier k is $P_{p,k}$. We assume that Φ_k follows an independent homogeneous PPP with density λ_k, $k \in \{1, 2, \cdots, K\}$. The UEs obey a homogeneous PPP Φ_u with density λ_u, which is independent of Φ_k. We assume that λ_u is large enough so that each BS serves at least one associated UE per channel. That is, the uplink channels are fully occupied as in high traffic load conditions.

A. Path Loss and Association Policy

We consider both small- and large-scale propagation effects in the channel model. In particular, given a transmitter at
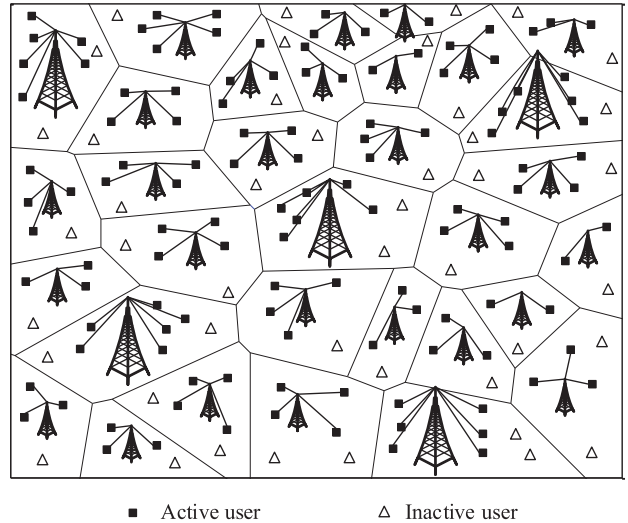
Fig. 1.   System model of a multi-tier HetNet.

$x \in \mathbb{R}^2$, the receiving power at $y \in \mathbb{R}^2$ is given by $P_{d,x} A h_{x,y} L^{-1}(x, y)$, where $P_{d,x}$ is the transmit power. A is a propagation constant. $h_{x,y}$ denotes the fading channel power due to multi-path propagation from x to y. Moreover, $L(x, y) = S_{x,y} \|x - y\|^\alpha$ models the channel variations caused by path loss $\|x - y\|^\alpha$ and shadowing effect $S_{x,y}$, where α is the path loss exponent and $\|x - y\|$ denotes the Euclidean distance between x and y. We consider Rayleigh multipath fading and log-normal shadowing, i.e., $h_{x,y} \sim \exp(1)$ is exponentially distributed with unit mean power and $\log_{10}(S_{x,y}/10)$ is a zero-mean Gaussian random variable. For deriving the analytical results, the path loss exponent α is assumed to vary rarely across different tiers.

Each UE associates to the BS that provides the maximum average received power. For example, the UE located at y is associated to the BS at x in tier k if and only if $P_{p,k} L^{-1}(x, y) \geq P_{p,j} L_{\min,j}^{-1}(y)$ for $j = 1, \cdots, K$. The resulting association is stationary [35], i.e., the association pattern is invariant under translation with any displacement. Note that since $P_{p,k}$ varies from tier to tier, the superposition of BSs in all tiers of the HetNets, denoted as $\Phi = \bigcup_k \Phi_k$, generally forms a multiplicatively weighted Poisson Voronoi tessellation [33]. According to the Palm theory [22], the analytical results of a typical cell C_0 in tier k can be extended to other cells C_i ($i = 1, 2, \cdots$) in the same tier. Therefore, we only need to focus on the cell C_0 for the analysis in the remainder of this paper.

The UEs are equipped with single antenna and access the network by using single-carrier FDMA (SC-FDMA) technique to avoid intra-cell interference [34]. However, due to the universal frequency reuse, the uplink transmission of UEs in one cell suffers co-channel interference from UEs in other cells. Let Φ_{u_o} be the point process of co-channel interfering UEs. As only one UE is allowed to operate on the typical frequency in each cell by SC-FDMA, Φ_{u_o} is a Poisson-Voronoi perturbed lattice process, which consists of a random point in each Voronoi cell [35].

The BSs in tier k have a receiving sensitivity $\rho_{\min,k}$, where the value of $\rho_{\min,k}$ can vary across tiers. For successful

data transmission, the UEs associated to the kth tier cells should keep the average received power at their associated BSs above $\rho_{\min,k}$. For this purpose, uplink power control is usually applied at the UEs, to keep the average received power at the BSs above the receiver threshold ρ_0, where $\rho_0 > \rho_{\min,k}$ for any tier k. Otherwise, the UEs will fall into a truncation outage due to the insufficient received power at BS.

B. Uplink Power Control

The total power consumption of a UE for transmission in the uplink is given by

$$P = P_s + P_{d,t}, \tag{1}$$

where P_s is the static power consumed in base-band signal processing and radio frequency (RF) circuits, independent of $P_{d,t}$. In contrast, $P_{d,t}$ denotes the dynamic power needed for wireless transmission. The maximum dynamic power consumption of UEs is limited by $P_{\max}$, i.e., $P_{d,t} \leqslant P_{\max}$, due to the limited battery storage at UEs and the operation requirement for power amplifiers in RF circuits.

In this paper, we consider distance-proportional FPC, or simply FPC, which is an open-loop scheme widely adopted in uplink transmission [13]. By FPC, the dynamic transmit power for the UE is set as

$$P_{d,t} = P_u(\varepsilon) L^\varepsilon(t, x), \tag{2}$$

where $\varepsilon \in [0, 1]$ is the power control coefficient. For problem tractability, we assume that all uplink UEs in the network use a uniform power control coefficient ε, whose value is to be controlled network-wide.[1] $L(t, x)$ is the path loss from UE at t to its associated BS at x. In (2), the path loss is partially compensated in general as $\varepsilon \in [0, 1]$. $P_u(\varepsilon)$ is the open-loop power spectral density and is set as $P_u(\varepsilon) = \rho_0^\varepsilon P_{\max}^{1-\varepsilon}$ [15].

Note that the FPC scheme includes two other schemes as special cases: i) when $\varepsilon = 0$, FPC reduces to the constant power control scheme, where all UEs in each cell transmit with the maximum output power $P_{\max}$; ii) when $\varepsilon = 1$, FPC becomes the power control scheme with complete channel inversion, i.e., the dynamic power consumption fully compensates the channel variations. Note that in the first case, there is no channel inversion and the dynamic power consumption is constant.

The maximal output power constraint is another realistic mechanism for uplink UEs. If UEs located at cell edges cannot overcome the path loss to their associated BS even by transmitting at their maximal output power, they will be truncated and fail to transmit signals. Therefore, the status of the UEs are divided as active and inactive. Fig. 1 shows that due to the limitation of maximal output power, some cell edge UEs will be inactive.

By adopting the FPC and the maximal transmit power constraint, the uplink UE becomes inactive when $L(t, x) \geqslant P_{\max}/\rho_0$. It is expected that the system with large $P_{\max}$ and/or small ρ_0 will enable a large access region for the uplink. Moreover, both $P_{\max}$ and ρ_0 can affect the transmit power,

[1]The general case of adopting non-uniform power control coefficients is more difficult to analyze and will be left for the future work.

Φ_k, λ_k	PPP of k-th tier BS and the corresponding density
Φ_u, λ_u	PPP of UEs and the corresponding density
Φ_{u_0}	Point process of co-channel interfering UEs
α	Path loss exponent
$P_{d,t}, P_s$	Dynamical transmit power and static power of uplink UE
$\varepsilon, P_u(\varepsilon)$	Power control coefficient, open loop power spectral density
$\rho_{\min,k}, \rho_0$	Receiver sensitivity of tier k, receiver threshold for FPC
$P_{\max}$	Maximal transmission power of uplink UE
$h_{x,y}, S_{x,y}$	Small and large scale fading between nodes located x and y
$P_{p,k}$	Pilot transmission power of BS in k-th tier
W, B	Total bandwidth and the bandwidth allocated to UE
N	Number of uplink UEs sharing the spectrum

and hence, play an important role in the analysis of uplink energy efficiency.

C. Energy Efficiency of Uplink UEs

We assume the BS in cell C_0 (termed the typical BS) is located at origin o and is denoted by BS_0. When a randomly chosen UE in cell C_0 (termed the typical UE) transmits its desired signal to BS_0, the receiving SINR of BS_0 is given by

$$SINR = \frac{P_{d,t} A h_{t,o} L_t^{-1}}{N_o + I_o}, \tag{3}$$

where $I_o = \sum_{x \in \Phi_{u\_o}} P_{d,x} A h_{x,o} L_x^{-1}$ is the aggregate interference power received at BS_0. $h_{t,o}$ and $h_{x,o}$ denote the power gains of the fading channels from the typical UE and the interfering UE at $x \in \Phi_{u\_o}$ to BS_0, respectively. N_o is the thermal noise power. Since BS_0 is located at the origin, we simply denote $L(t, o)$ and $L(x, o)$ as L_t and L_x, respectively.

Considering the FPC scheme, the SINR expression in (3) can be obtained as

$$SINR = \frac{h_{t,o} L_t^{\varepsilon-1}}{SNR^{-1} + \sum_{x \in \Phi_{u\_o}} h_{x,o} L^\varepsilon(x, b_x) L_x^{-1}}, \tag{4}$$

where $SNR = \frac{P_u(\varepsilon) A}{N_o}$ and b_x is the location of the associated BS for the interfering UE located at $x \in \Phi_{u\_o}$. Moreover, the achievable transmission rate of the desired uplink UE is

$$R = B \log_2(1 + SINR), \tag{5}$$

where B is the bandwidth allocated for the UE. Taking into account the UE power consumption model in (1), the energy efficiency of a UE in the uplink is then defined as the ratio of the achievable rate to the power consumption, i.e.,

$$\eta = \frac{R}{P} = \frac{B \log_2(1 + SINR)}{P_s + P_{d,t}}. \tag{6}$$

The notations used in this paper are listed in Table I.

III. UPLINK ENERGY EFFICIENCY IN DIFFERENT PATH LOSS REGIMES

In this section, we evaluate the uplink energy efficiency of the typical UE, assuming that the locations of BSs and UEs are fixed. This corresponds to a particular realization of the stochastic geometry HetNets as studied in Section II.

We reveal the properties of uplink energy efficiency for different path loss regimes qualitatively. The optimal power control coefficient for maximizing the uplink energy efficiency of UEs is also obtained. For obtaining analytical insights, we assume throughout this section that the receiver threshold at BS is relative low compared to P_{max} such that the maximal transmit power constraint becomes inactive. We note that the derivations in this section do not rely on the PPP assumptions, and hence, the results hold for arbitrarily distributed Φ_k and Φ_u.

A. Transfer Path Loss and Energy Efficiency

In this subsection, we detail the energy efficiency analysis for the proposed uplink model with FPC. We show several interesting properties of uplink energy efficiency as the path loss and the power control coefficient are varied.

The deterministic analysis in this section is motivated by the asymptotic behavior of energy efficiency in the high path loss regime, i.e., $l \to \infty$. Let l be the path loss between the typical UE and its associated BS. Substituting (2) and (4) into (6), the energy efficiency of the UE is given by

$$\eta(l, \varepsilon) = \frac{B\log_2\left(1 + \frac{h_{t,o}l^{\varepsilon-1}}{SNR^{-1} + \sum_{x \in \Phi_{u\_o}} L^\varepsilon(x, b_x)h_{x,o}L_x^{-1}}\right)}{P_u(\varepsilon)l^\varepsilon + P_s}. \quad (7)$$

Note that, when the receiver threshold is low, l can be large without causing truncation outage as $L_{max} \leq P_{max}/\rho_0$. In the high path loss regime, the dynamic power consumption, which scales with the path loss and the power control coefficient, will dominate the total power consumption since $P_s \ll P_u(\varepsilon)l^\varepsilon$. Therefore, the static power consumption P_s can be ignored such that $P_u(\varepsilon)l^\varepsilon + P_s \approx P_u(\varepsilon)l^\varepsilon$ (this condition also holds for $\varepsilon = 0$ since $P_u(\varepsilon) = P_{max}$ is typically around 1 W while P_s is just tens of mW.). If $\epsilon \in [0, 1)$, $h_{t,o}l^{\varepsilon-1}$ is small such that the energy efficiency $\eta(\varepsilon, l)$ can be approximated as

$$\lim_{l \to \infty} \eta(l, \varepsilon) = \frac{Bh_{t,o}l^{-1}\log_2 e}{P_u(\varepsilon)\left(SNR^{-1} + \sum_{x \in \Phi_{u\_o}} L^\varepsilon(x, b_x)h_{x,o}L_x^{-1}\right)}, \quad (8)$$

where $\ln(1 + x) \approx x$ for $x \to 0$. On the other hand, if $\varepsilon = 1$, we have

$$\eta(l, \varepsilon) \approx \frac{Bl^{-1}}{P_u(\varepsilon)}\log_2\left(\frac{h_{t,o}}{SNR^{-1} + \sum_{x \in \Phi_{u\_o}} L(x, b_x)h_{x,o}L_x^{-1}}\right).$$

Therefore, when uplink UE is far away from its associated BS, the uplink energy efficiency always changes as $O(l^{-1})$ for any $\varepsilon \in [0, 1]$. Without loss of generality, we write $\lim_{l \to \infty} \eta(l, \varepsilon) = \frac{N(l)}{D(\varepsilon)}$, where $N(l)$ is set as the numerator of (8) and $D(\varepsilon)$ is chosen accordingly for specific value of ε.

In (8), we have set $l \to \infty$ for mathematical tractability. In the following, we will evaluate the energy efficiency in the finite path loss regime and characterize the range of path losses, i.e., how large should l be, such that (8) holds.

In particular, to study the impact of power control coefficient on uplink energy efficiency of UEs using simplified notations, the relative energy efficiency is applied, which is defined as the ratio of $\eta(l, \varepsilon)$ to $\eta(l, 0)$, i.e.,

$$r\_\eta(l, \varepsilon) = \frac{\eta(l, \varepsilon)}{\eta(l, 0)}. \quad (9)$$

Thereby, $r\_\eta(l, \varepsilon)$ gives the energy efficiency of adopting power control coefficient ε at UEs relative to $\eta(l, 0)$, which is the energy efficiency of applying the constant power control scheme. As a trivial result, $r\_\eta(l, \varepsilon) = 1$ holds if $\varepsilon = 0$.

According to (8) and (9), we have $r\_\eta(l, \varepsilon) = \frac{D(0)}{D(\varepsilon)}$ as $l \to \infty$. That is, the relative energy efficiency remains constant for given ε in the high path loss regime. The properties of the relative energy efficiency are detailed below.

Property 1: For any $0 < \varepsilon \leq 1$, the intersection point between $r\_\eta(l, \varepsilon)$ and $D(0)/D(\varepsilon)$ is $l^* = \left(\frac{I(\varepsilon)}{I(0)}\right)^{1/\varepsilon}$, where

$$I(\varepsilon) = \frac{D(\varepsilon)}{P_u(\varepsilon)} = SNR^{-1} + \sum_{x \in \Phi_{u,o}} L^\varepsilon(x, b_x)h_{x,o}L_x^{-1}. \quad (10)$$

Proof: The intersection point of $r\_\eta(l, \varepsilon)$ and $D(0)/D(\varepsilon)$ is obtained by solving the equation $r\_\eta(l, \varepsilon) = D(0)/D(\varepsilon)$. According to (7) and (10), we obtain

$$\left[\frac{\log_2\left(1 + h_{t,o}l^{(\varepsilon-1)}/I(\varepsilon)\right)}{P_u(\varepsilon)l^\varepsilon}\right] \Bigg/ \left[\frac{\log_2\left(1 + h_{t,o}l^{-1}/I(0)\right)}{P_u(0)}\right]$$
$$= \frac{P_u(0)I(0)}{P_u(\varepsilon)I(\varepsilon)}. \quad (11)$$

That is, $l^{-\varepsilon} \cdot \log_2\left(1 + h_{t,o}l^{(\varepsilon-1)}/I(\varepsilon)\right) = \frac{I(0)}{I(\varepsilon)} \cdot \log_2\left(1 + h_{t,o}l^{-1}/I(0)\right)$.

According to Taylor's theorem, for $|x| < 1$, $\log_2(1 + x) \approx \log_2 e\left(x + \frac{x^2}{2} + O(x^2)\right)$. Since the path loss of UE l is large enough such that $h_{o,b_0}l^{(\varepsilon-1)}/I(\varepsilon) < 1$, (11) reduces to $l^{(\varepsilon-1)}I(0) = I(\varepsilon)l^{-1}$, whose solution is given by $l^* = \left(\frac{I(\varepsilon)}{I(0)}\right)^{1/\varepsilon}$. This completes the proof. $\blacksquare$

We refer to l^*, which is the intersection of relative energy efficiency and $D(0)/D(\varepsilon)$, as the *transfer path loss*. In the sequel, the transfer path loss defines a critical point for inspecting the uplink energy efficiency of UEs, based on which the typical cell can divided into two access regions with different behaviors in terms of energy efficiency. Before that, an upper bound and a lower bound of l^* are readily available.

Theorem 1: When the noise power is negligible compared to the interference power, the transfer path loss l^* is bounded by

$$\frac{\sum_{x \in \Phi_{u\_o}} h_{o,x}L_x^{-1}}{\sum_{x \in \Phi_{u\_o}} L^{-\varepsilon}(x, b_x)h_{o,x}L_x^{-1}} \leq (l^*)^\varepsilon \leq \mathbb{E}\left[L^\varepsilon(x, b_x)\right].$$

Proof: By ignoring the noise in $I(\varepsilon)$, $I(\varepsilon)/I(0)$ is given as

$$\frac{I(\varepsilon)}{I(0)} = \frac{\sum_{x \in \Phi_{u\_o}} L^\varepsilon(x, b_x)h_{o,x}L_x^{-1}}{\sum_{x \in \Phi_{u\_o}} h_{o,x}L_x^{-1}}. \quad (12)$$

$$\frac{I\left(\varepsilon\right)}{I\left(0\right)} = \exp\left[\ln\left(\sum_{x\in\Phi_{u\_o}} L^{\varepsilon}\left(x,b_x\right)h_{o,x}L_x^{-1}\right) - \ln\left(\sum_{x\in\Phi_{u\_o}} h_{o,x}L_x^{-1}\right)\right] \tag{13}$$

For $0 \le \varepsilon \le 1$ and $x > 0$, $a\left(x\right) = x^{\varepsilon}$ is a mono-increasing function of x, and $b\left(x\right) = x^{-1}$ is a mono-decreasing function of x. According to the Chebyshev's sum inequality [35], for any $a_k > 0$, $b_k > 0$ and sequences $\{a_k\}$, $\{b_k\}$ have different monotonicity properties, then $\frac{1}{n}\sum_{k=1}^{n} a_k b_k \leqslant \left(\frac{1}{n}\sum_{k=1}^{n} a_k\right)\left(\frac{1}{n}\sum_{k=1}^{n} b_k\right)$.

Hence, $\frac{I(\varepsilon)}{I(0)} \leqslant \frac{1}{n}\sum_{x\in\Phi_{u\_o}} L^{\varepsilon}\left(x,b_x\right)$, where n is the number of interfering UEs. According to Property 1, $\left(l^*\right)^{\varepsilon} = I\left(\varepsilon\right)/I\left(0\right)$. Therefore, the upper bound is obtained as $\left(l^*\right)^{\varepsilon} \leqslant \frac{1}{n}\sum_{x\in\Phi_{u\_o}} L^{\varepsilon}\left(x,b_x\right) = \mathbb{E}\left[L^{\varepsilon}\left(x,b_x\right)\right]$.

To derive the lower bound, we first observe (13), shown at the top of this page. Since $\ln x$ is a concave function of x, it can be obtained as

$$\ln\left(\sum_{x\in\Phi_{u\_o}} L^{\varepsilon}\left(x,b_x\right)h_{o,x}L_x^{-1}\right) - \ln\left(\sum_{x\in\Phi_{u\_o}} h_{o,x}L_x^{-1}\right)$$

$$> \ln\left(\sum_{x\in\Phi_{u\_o}} h_{o,x}L_x^{-1}\right) - \ln\left(\sum_{x\in\Phi_{u\_o}} L^{-\varepsilon}\left(x,b_x\right)h_{o,x}L_x^{-1}\right). \tag{14}$$

which leads to inequality $\frac{I(\varepsilon)}{I(0)} > \frac{\sum_{x\in\Phi_{u\_o}} h_{o,x}L_x^{-1}}{\sum_{x\in\Phi_{u\_o}} L^{-\varepsilon}(x,b_x)h_{o,x}L_x^{-1}}$. Therefore, the lower bound of $\left(l^*\right)^{\varepsilon}$ is given by $\frac{\sum_{x\in\Phi_{u\_o}} h_{o,x}L_x^{-1}}{\sum_{x\in\Phi_{u\_o}} L^{-\varepsilon}(x,b_x)h_{o,x}L_x^{-1}}$. This completes the proof. ■

The lower and upper bounds in Theorem 1 also reveal the impact of interfering UEs on the transfer path loss. Note that the upper bound of $\left(l^*\right)^{\varepsilon}$ gives the expected εth moment of $L\left(x,b_x\right)$, while the lower bound of $\left(l^*\right)^{\varepsilon}$ is the inverse of the generalized abstracted mean value of moment $L^{\varepsilon}\left(x,b_x\right)$ [38]. That is, the transfer path loss of l^* is fundamentally determined by the moment of $L\left(x,b_x\right)$. This is because, by FPC, the path loss between an interfering UE and its associated BS, i.e., $L\left(x,b_x\right)$, determines the average interference power, cf. (4). Since UEs in the regime of high path loss usually locate far from their associated BS, the uplink energy efficiency of these UEs is sensitive to the interference power.

The transfer path loss provides an interesting starting point for energy efficiency analysis. In particular, as revealed in Properties 2 and 3, the energy efficiency exhibits adverse behaviors in different access regions divided according to the transfer path loss.

Property 2: In the access region of $l > l^*$, $\eta\left(l,\varepsilon\right)$ is closely approximated by $N\left(l\right)/D\left(\varepsilon\right)$, where the maximal gap between $\eta\left(l,\varepsilon\right)$ and $N\left(l\right)/D\left(\varepsilon\right)$ is bounded by $N\left(l^*\right)P_u^{-1}\left(\varepsilon\right)I^{-2}\left(\varepsilon\right)\cdot h_{t,o}l^{*(\varepsilon-1)}$.

Proof: Please refer to Appendix A. ■

Remark 1: Based on Property 2, if the path loss of UE satisfies $l > l^*$, the uplink energy efficiency of UE scales with l as $O\left(l^{-1}\right)$ approximately. This implies that $l > l^*$ is sufficiently large for (8) to hold. Specifically, even though in

the finite path loss regime of $l^* < l < \infty$, the system is interference limited, and the SINR of the desired UE is low such that the approximation $\ln\left(1+x\right) \approx x$ in (8) is valid. Hence, the uplink energy efficiency scales with path loss in the order of $O\left(l^{-1}\right)$. Note that for $l > l^*$, $D\left(\varepsilon\right)$ is a monotonically increasing function of ε, and a small ε always leads to a high uplink energy efficiency for given path loss l, independent of the value of path loss. Hence, for $l > l^*$, the optimal power control coefficient will always be zero. This is expected as, if a UE is far away from its serving BS, its desired signals will be mainly degraded by the aggregate interference power from co-channel UEs in other cells. By decreasing the value of power control coefficient, the co-channel interference power reduces, and the energy efficiency of desired uplink UEs is improved.

Property 3: In the access region of $l < l^*$, $\eta\left(l,\varepsilon\right)$ is a mono-decreasing function of l and $\frac{\partial\eta(l,\varepsilon)}{\partial l}$ is a mono-increasing function of ε.

Proof: Please refer to Appendix B. ■

Remark 2: Property 3 is due to the fact that when UEs are close to the BS, the impact of interfering UEs on the desired uplink UEs becomes sufficiently weak, whereas the uplink energy efficiency in this region is critically determined by the power consumption of UE. In particular, the desired uplink UE can transmit its desired signal with a high data rate while consuming a small amount of power. The closer to its associated BS the desired UE is, the less dynamic transmit power is consumed. Therefore, the uplink energy efficiency decreases with path loss. Meanwhile, according to (2), the power consumption of UE decreases fast with large power control coefficient for given path loss. As a result, the uplink energy efficiency can increase with the power control coefficient at an increasing rate.

To verify the derivations above and, at the same time, to study the impact of path loss and power control coefficient on energy efficiency of uplink UE, Monte Carlo simulation results and analytical results are compared for different values of ε in Fig. 2. The same simulation parameters as in Table II of Section V are adopted here. Both analytical and simulation results show the existence of the transfer path loss for uplink energy efficiency. This is because, when UEs are located further than l^*, their energy efficiency curves for given ε become approximately parallel to the curve $\eta\left(l,0\right)$, i.e., they decrease inversely with the path loss, which is consistent with Property 2. On the other hand, when $l < l^*$, both power control coefficient and path loss can affect the uplink energy efficiency as established in Property 3.

Fig. 2 also provides insights into the impact of the co-channel interference on the uplink energy efficiency. In the region $l > l^*$, due to the influence from interfering UEs in other cells, the desired signal power and the interference power change in pace as $O(l^{\varepsilon-1})$ and $O(l^{\varepsilon})$ for different values of ε, respectively. Therefore, the resulting uplink energy efficiency

TABLE II
PARAMETERS SETTING FOR SIMULATIONS

Symbol	Default Value	Symbol	Default Value
$P_{\max}$	1W	λ_1	$2 \times 10^{-7}/\text{m}^2$
W	10 MHz	λ_2	$4 \times 10^{-7}/\text{m}^2$
α	4	μ_1	0 dB
σ^2	-90 dBm	μ_2	0 dB
P_1	41 dBm	S_1	4 dB
P_2	33 dBm	S_2	4 dB
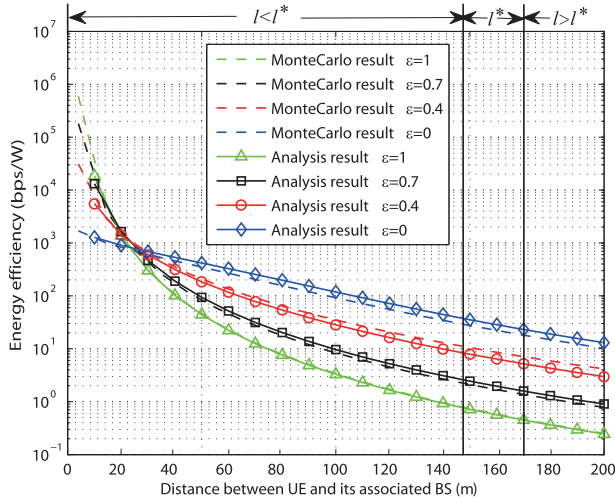
Fig. 2.   The analysis and numerical results of uplink energy efficiency changing with path loss for different power control coefficients. For l^*, the derived upper and lower bounds are also shown in the figure.

Fig. 3.   The optimal power control coefficient for maximization of uplink energy efficiency under different path losses.

decreases asymptotically as $O\left(l^{-1}\right)$ for given $\varepsilon \in [0, 1]$. In the region of $l < l^*$, however, interference power is relatively small since the desired UE is close to its associated BS. As a result, the uplink energy efficiency is mainly affected by the desired signal power. And UEs with small path loss and large power control coefficient will obtain a high uplink energy efficiency as the desired signal power is reduced.

B. Optimal Power Control Coefficient

Now we study the optimal power control coefficient for UEs in different access regions. Property 2 reveals that the uplink energy efficiency decreases with ε when path loss of UE satisfies $l > l^*$. Moreover, based on Property 3, the uplink energy efficiency increases rapidly with l in the region $l < l^*$ for large ε. Therefore, the optimal power control coefficient ε^* for maximizing uplink energy efficiency is $\varepsilon^* = 0$ when UEs is located in $l > l^*$. However, in the region of $l < l^*$, ε^* depends on the location of uplink UEs, which is further studied here. Without loss of generality, the uplink energy efficiency optimization problem can be formulated as

$$\max_{\varepsilon} \ \eta\left(\varepsilon, l\right)$$
$$\text{s.t. } 0 \leqslant \varepsilon \leqslant 1. \tag{15}$$

For given path loss l, the optimal ε^* in (15) can be obtained via one-dimensional search [39]. For example, given the path loss l, a simple uniform search can be applied, where the initial

interval of $I_0 = [0, 1]$ is equally divided into n small subintervals and the energy efficiency at grid points $\varepsilon_{0,k} = k/n$, $k = 0, \dots, n$, are evaluated. Let ε_0^* be the grid point achieving the largest value of $\eta\left(\varepsilon_{0,k}, l\right)$, it follows that the maximum of $\eta\left(\varepsilon, l\right)$ will lie in the interval $I_1 = \left[\varepsilon_0^* - 1/n, \varepsilon_0^* + 1/n\right]$ [33]. The process repeats by setting $I_0 = I_1$ before the desired accuracy is reached. The optimal power control coefficient for maximizing the uplink energy efficiency with different path losses is illustrated in Fig. 3. From Fig. 3 it can be observed that, when the path loss is small, the optimal power control coefficient is $\varepsilon^* = 1$, that is, the complete channel inversion power control will achieve the highest uplink energy efficiency. This result is consistent with Property 3. On the other hand, when the path loss of UE increases, so does the dynamic power consumption under complete channel inversion power control, which decreases the uplink energy efficiency. In this case, decreasing the power control coefficient can improve the energy efficiency for uplink UEs. When UE is far enough from its associated BS and the energy efficiency becomes mainly affected by the aggregate interference power, $\varepsilon^* = 0$ leads to the minimal interference power and therefore obtains the maximal uplink energy efficiency.

As analytical expressions of the optimal power control coefficient for solving (15) are generally difficult to obtain,[2] we will characterize $l^*(\varepsilon)$ alternatively. Herein, $l^*(\varepsilon)$ defines the path loss when the optimal uplink energy efficiency in (15) is achieved by employing power control coefficient ε. The upper bound of $l^*(0)$ and the lower bound of $l^*(1)$ are provided in Theorem 2. The derived results enable the power control policy to be adjusted in a convenient way for energy efficient uplink transmission.

Theorem 2: In the region $l < l^*(1)$, the optimal power control coefficient is $\varepsilon^* = 1$ and the lower bound of $l^*(1)$ is

---

[2]The approximation technique in [32] for deriving approximate optimal transmission capacity of FPC does not apply here as the energy efficiency optimization involves solving a fractional program, which is non-convex and hard to solve.

$\exp\left(\left(\frac{h_{o,b_0}I(1)}{\ln\left(1+h_{o,b_0}I(1)\right)}-1\right)^{-1}\cdot\frac{I'(1)}{I(1)}\right)$. In the region $l > l^*(0)$, the optimal power control coefficient is $\varepsilon^* = 0$ and the upper bound of $l^*(0)$ is $\frac{h_{t,o}I^{-1}(0)}{\ln\left(1+h_{t,o}I^{-1}(0)\right)}$.

Proof: Please refer to Appendix C. ∎

IV. AVERAGE UPLINK ENERGY EFFICIENCY UNDER MAXIMAL POWER CONSTRAINT

When the maximal transmit power constraint is taken into account, the uplink energy efficiency becomes dependent on the receiver threshold. For example, if the BSs have a large receiver threshold, although the energy efficiency of the active UEs can be high, the number of active UEs will decrease, i.e., more UEs will suffer truncation outage. On the other hand, if the receiver threshold of BS is small so that more associated UEs are active, then UEs with bad channels and thus low energy efficiency will deteriorate the average uplink energy efficiency in the HetNets. Therefore, under the maximal transmit power constraint, the average uplink energy efficiency of all UEs has to be investigated. Different from the deterministic analysis in Section III, the spatial distributions of BSs and UEs (following independent PPPs, cf. Section II), are considered for a quantitative evaluation of the average energy efficiency. With the aid of stochastic geometric theory, we first characterize the probability distributions of transmit power and the truncation outage probability. Based on these results, we could then derive the average energy efficiency in the uplink.

A. Distribution of Path Loss

We define the propagation process from the typical UE to its serving BS in tier k as $U_c \triangleq \{L(o,t)\}_{o\in\Phi_k}$. The process U_c can be interpreted as an inhomogeneous Poisson point process with intensity measure $\Lambda_k(t) = \pi\lambda_k\mathbb{E}\left[S_k^{2/\alpha}\right]t^{2/\alpha}$ [29], which varies with tier index k. Then, based on U_c, we characterize in Proposition 1 the distribution of the path loss between UEs and their associated BSs.

Proposition 1: Under maximum transmission power constraint, the probability density function (PDF) of the path loss between a typical active UE and its serving BS is given by

$$f_{L\le L_{\max}}(l) = \delta l^{\delta-1}\sum_{j=1}^{K}\frac{\pi\lambda_j\mathbb{E}\left[S_j^\delta\right]\cdot\exp\left(-G_jl^\delta\right)}{1-\exp\left(-G_jL_{\max}^\delta\right)},\quad(16)$$

for $0 \le l \le L_{\max}$, where $\delta = 2/\alpha$ and $G_k = \sum_{j=1}^{K}\pi\lambda_j\mathbb{E}\left[S_j^\delta\right]\left(P_{p,j}/P_{p,k}\right)^\delta$ denotes the superposition intensity of BSs.

Proof: Define $A_k = P(\mathcal{K}=k)$ as the probability of selecting tier k during UE and BS association, where $\mathcal{K}$ is a random variable to denote the associated tier of the typical UE. We have [33]

$$A_k = \frac{\lambda_k\mathbb{E}\left[S_k^\delta\right]P_{p,k}^\delta}{\sum_{j\in K}\lambda_j\mathbb{E}\left[S_j^\delta\right]P_{p,j}^\delta}.\quad(17)$$

The PDF of path loss between the typical UE and its associated BS in tier k is obtained by the derivative of $\Lambda_k(t)$ [29] as

$$f_L(l\mid\mathcal{K}=k) = \delta G_kl^{\delta-1}\exp\left(-G_kl^\delta\right).\quad(18)$$

Under the maximal transmit power constraint, the path loss of the active UE is limited by $L_{\max} = P_{\max}/\rho_0$. Therefore, under maximum output power constraint, the conditional path loss distribution for the desired uplink UE that associates to tier k is

$$\begin{aligned}f_{L\le L_{\max}}(l\mid\mathcal{K}=k) &= \frac{f_L(l\mid\mathcal{K}=k)}{\mathbb{P}(l\le L_{\max})}\\ &= \frac{\delta G_kl^{\delta-1}\cdot\exp\left(-G_kl^\delta\right)}{\int_0^{L_{\max}}\delta G_kr^{\delta-1}\cdot\exp\left(-G_kr^\delta\right)dr}\\ &= \frac{\delta G_kl^{\delta-1}\cdot\exp\left(-G_kl^\delta\right)}{1-\exp\left(-G_kL_{\max}^\delta\right)}.\end{aligned}\quad(19)$$

Based on (17) and (19), the path loss distribution for the desired uplink can be obtained based on the total probability formula as

$$\begin{aligned}f_{L\le L_{\max}}(l) &= \sum_{j=1}^{K}A_j\frac{\delta G_jl^{\delta-1}\cdot\exp\left(-G_jl^\delta\right)}{1-\exp\left(-G_jL_{\max}^\delta\right)}\\ &= \delta l^{\delta-1}\sum_{j=1}^{K}\frac{\pi\lambda_j\mathbb{E}\left[S_j^\delta\right]\cdot\exp\left(-G_jl^\delta\right)}{1-\exp\left(-G_jL_{\max}^\delta\right)}.\end{aligned}$$
∎

Corollary 1: Assume that the typical UE is associated to tier k, i.e., $\mathcal{K}=k$. Let random variable $\mathcal{K}_I$ denote the associated tier for a subset of interfering UEs, e.g., $\mathcal{K}_I = j$ denotes interfering UEs in tier j. The path loss between an interfering UE at x and the typical BS is given as $L(x,o) = y$. Then, under the maximal transmit power constraint, the conditional PDF of the path loss between the interfering UE and its associated BS in tier j, denoted by $L(x,b_x)$, is given as

$$\begin{aligned}&f_{L_I\le L_{\max}}(l_I\mid\mathcal{K}_I=j,\mathcal{K}=k,L(x,o)=y)\\ &= \frac{\delta G_jl_I^{\delta-1}\cdot\exp\left(-G_jl_I^\delta\right)}{\left(1-\exp\left(-G_jL_{\max}^\delta\right)\right)\left(1-\exp\left(-G_ky^\delta\right)\right)}.\end{aligned}\quad(20)$$

Proof: According to the association rule, the interfering UE cannot associate with tier k and its path loss is bounded as $L(x,b_x) \le \frac{P_{p,j}}{P_{p,k}}L(x,b_0)$. According to the definition of G_k, we can obtain $G_k = G_j\left(\frac{P_{p,j}}{P_{p,k}}\right)^\delta$. Then the path loss distribution for interfering UEs associated with BSs in tier j is

$$\begin{aligned}&f_{L_I\le L_{\max}}(l_I\mid\mathcal{K}_I=j,\mathcal{K}=k,L(x,b_0)=y)\\ &= \frac{f_L(l_I\mid\mathcal{K}_I=j,\mathcal{K}=k)}{\mathbb{P}\left(l_I\le\frac{P_jy}{P_k}\right)}\\ &= \frac{\delta G_jl_I^{\delta-1}\cdot\exp\left(-G_jl_I^\delta\right)}{\left(1-\exp\left(-G_jL_{\max}^\delta\right)\right)\left(1-\exp\left(-G_ky^\delta\right)\right)}.\end{aligned}\quad(21)$$
∎

Based on (19) and (21) we observe that, if the path loss between an interfering UE at x and the typical BS in tier k at o is $L(x,o)$, then the interfering UE associates to its

serving BS in tier k with probability $\exp\left(-G_k L^\delta(x, o)\right)$ while it associates to the BS in other tiers with probability $\left[1 - \exp\left(-G_k L^\delta(x, o)\right)\right]$. A similar property was also found in [30]; however, here we show it for uplink power control with constrained transmit power. Based on this property, when the typical BS is located in tier k, the propagation process of interfering UEs in tier j to the location of the typical BS can be approximated by a PPP. Corollary 1 also implies that the path loss distribution of the interfering UEs in tier k is thinned from the parent path loss distribution of the desired UEs in (16) or (19) with probability $\left[1 - \exp\left(-G_k L(x, o)\right)\right]$. This thinning property regarding the point process of interfering UEs is also described in [31] by applying an exponent approximation method. Although the approximation method in [31] achieves a high accuracy, the complexity is very high for multi-tier HetNets. Hence, for low computational complexity, we only use the general thinning factor in this paper.

B. Distribution of Transmit Power

Based on Proposition 1, we can further obtain the PDF of transmit power.

Proposition 2: Under maximal transmit power constraint, the PDF of the transmit power for an active UE in tier k is

$$f_{P_{d,k} \leq P_{\max}}(x \mid \mathcal{K} = k) = \frac{\delta G_k x^{\delta/\varepsilon - 1} \exp\left(-G_k \left(\frac{x}{P_u(\varepsilon)}\right)^{\delta/\varepsilon}\right)}{\varepsilon P_u^{\delta/\varepsilon}(\varepsilon)\left(1 - \exp\left(-G_k L_{\max}^\delta\right)\right)},$$

$$(22)$$

for $0 \leq x \leq P_{\max}$.

Proof: For an active UE in tier k, the transmit power is given by $P_{d,k} = P_u(\varepsilon) L_{t,k}^\varepsilon$, where $L_{t,k}$ has the Rayleigh distribution as shown in (18). The PDF of $P_{d,k}$ is then given by

$$f_{P_{d,k} \leq P_{\max}}(x \mid \mathcal{K} = k)$$

$$= \frac{\delta G_k x^{\delta/\varepsilon - 1} \cdot \exp\left(-G_k\left(x/P_u(\varepsilon)\right)^{\delta/\varepsilon}\right)}{\varepsilon P_u^{\delta/\varepsilon}(\varepsilon) \int_0^{P_{\max}} \delta G_k t^{\delta/\varepsilon - 1} \cdot \exp\left(-G_k\left(t/P_u(\varepsilon)\right)^{\delta/\varepsilon}\right) dt}$$

$$= \frac{\delta G_k x^{\delta/\varepsilon - 1} \cdot \exp\left(-G_k\left(x/P_u(\varepsilon)\right)^{\delta/\varepsilon}\right)}{\varepsilon P_u^{\delta/\varepsilon}(\varepsilon)\left(1 - \exp\left(-G_k L_{\max}^\delta\right)\right)}. \tag{23}$$

This completes the proof. However, as a byproduct of the proof, we obtain the μth moment of $P_{d,k}$ as $\mathbb{E}\left[P_{d,k}^\mu\right] = \int_0^{P_{\max}} x^\mu f_{P_{d,k}}(x)\, dx$, and

$$\mathbb{E}\left[P_{d,k}^\mu\right] = \int_0^{P_{\max}} \frac{\delta G_k x^{\delta/\varepsilon + \mu - 1} \exp\left(-G_k\left(\frac{x}{P_u(\varepsilon)}\right)^{\delta/\varepsilon}\right)}{\varepsilon P_u^{\delta/\varepsilon}(\varepsilon)\left(1 - \exp\left(-G_k L_{\max}^\delta\right)\right)} dx$$

$$= \frac{P_u^\mu(\varepsilon)\, \gamma\left(\mu\varepsilon/\delta + 1, G_k L_{\max}^\delta\right)}{G_k^{\mu\varepsilon/\delta}\left(1 - \exp\left(-G_k L_{\max}^\delta\right)\right)}, \tag{24}$$

which will enable us to explain the simulation results in Section V. ∎

Based on Proposition 2, for given power control coefficient ε, the average transmit power of UEs decreases with $L_{\max}$. This is because a large $L_{\max}$ allows the uplink UEs to transmit at a high power level. Meanwhile,

Proposition 2 shows that the average transmission power of uplink UEs decreases with the superposition intensity of BSs G_k. This is reasonable since the average path loss between a UE and its associated BS decreases with G_k. Thus the UE only requires a lower transmit power to overcome the path loss attenuation.

C. Truncation Outage Probability

The typical UE associated to BSs in tier k possibly suffer truncation outage due to the maximal transmit power constraint. The truncation outage probability, defined as $P_{out} \triangleq \sum_{j=1}^K A_j \cdot P_{out}(\mathcal{K} = k)$, is characterized in the following proposition.

Proposition 3: The truncation outage probability P_{out} of uplink UEs associated with multi-tier cellular networks is

$$P_{out} = \sum_{j=1}^K A_j \exp\left(-G_j\left(P_{\max}/\rho_0\right)^\delta\right). \tag{25}$$

Proof: According to the path loss distribution given in Proposition 1, the truncation outage probability of uplink UEs associated to tier k is obtained as

$$P_{out}(\mathcal{K} = k) \triangleq \mathbb{P}\left\{L_t \geq \frac{P_{\max}}{\rho_0}\right\} = \exp\left(-G_k\left(P_{\max}/\rho_0\right)^\delta\right).$$

Then, by applying the total probability formula and the probability of tier selection, (25) is readily available. ∎

From Proposition 3 we can observe that the truncation outage probability increases with ρ_0. This is due to the fact that the smaller the receiver threshold is, the more uplink UEs will become active, which can reduce the truncation outage probability. However, the active UEs with bad channels may deteriorate the uplink energy efficiency in HetNets. Hence ρ_0 leverages a trade-off between the average uplink energy efficiency and the truncation outage probability in the K-tier HetNets, which will be investigated in the sequel.

D. Average Uplink Energy Efficiency

Assume that the spectrum bandwidth is equally allocated among the UEs associated to the typical BS, the average uplink energy efficiency in the HetNets is then given by

$$\mathbb{E}[\eta] = \mathbb{E}\left[\frac{W}{N} \cdot \frac{\log(1 + SINR)}{(P_s + P_{d,t})}\right], \tag{26}$$

where W is the total bandwidth of spectrum, N is the total number of uplink UEs sharing the spectrum resource. The average uplink energy efficiency of the HetNets is characterized by the following theorem.

Theorem 3: The average uplink energy efficiency of active UEs with power control coefficient ε under maximum transmit power constraint is given by (27), shown at the bottom of the next page, where $\tau = 2^{\eta n\left(P_s + P_{d,t}\right)/W} - 1$, $\mathbb{P}(N = n) = \frac{3.5^{3.5}}{(n-1)!} \frac{\Gamma(n+3.5)}{\Gamma(3.5)}\left(\frac{\lambda_u A_k}{\lambda_k}\right)^{n-1}\left(3.5 + \frac{\lambda_u A_k}{\lambda_k}\right)^{-(n+3.5)}$, $_2F_1(\cdot)$ denotes the Gauss hypergeometric function [40], and $\mathbb{E}_{L_1 \mid \mathcal{K} = k}[x]$ is given in Corollary 1.

Proof: According to the total probability formula, the average uplink energy efficiency of UEs in K-tier HetNets is given by

$$\mathbb{E}[\eta] = \sum_{k=1}^{K} A_k \mathbb{E}_k[\eta \,|\, \mathcal{K} = k], \qquad (28)$$

where A_k is the probability that uplink UEs are associated with BSs in tier k. $\mathbb{E}[\eta \,|\, \mathcal{K} = k]$ is the average energy efficiency given that the uplink UEs are associated with BSs in tier k. From (17), we have (29), shown at the bottom of this page, where $\mathbb{P}(N = n)$ is the probability mass function (PMF) for the random number of uplink UEs associated to tier k [41].

Substituting (4) into (29), we have (30), shown at the bottom of this page, where (a) is due to Rayleigh fading $h_{t,o} \sim \exp(1)$. $I_r = \sum_{x \in \Phi_{u\_o}} h_{x,o} L^{\varepsilon}(x, b_x) L_x^{-1}$ is the uplink interference at the BS_0. Finally, $\mathcal{L}_{I_r | k_{BS} = k, N = n}(s)$ is the Laplace transform of the interference when the serving BS is located in tier k and the load number is n.

Considering the maximal transmit power for the active UE, we have

$$\mathbb{E}\left[\exp\left(-\tau L_x^{1-\varepsilon} SNR^{-1}\right)\right]$$
$$= \int_0^{L_{\max}} \exp\left(-\tau l^{1-\varepsilon} SNR^{-1}\right) f_L(l \,|\, \mathcal{K} = k) \, dl, \quad (31)$$

where $f_L(l \,|\, \mathcal{K} = k)$ is given in (18). Moreover, the Laplace transform of interference $\mathcal{L}_{I_r | k_{BS} = k}(s)$ under an

inhomogeneous PPP model can be obtain from [30] as (32), shown at the bottom of the this page.

Finally, (27) can be obtained by substituting (30), (31), and (32) into (29). This completes the proof. ∎

V. PERFORMANCE EVALUATION

In this section, the derived analytical results are validated via Monte Carlo simulation and the impact of power control coefficient, dynamic power consumption and density of BS on the system performance is also evaluated. We consider a two-tier HetNet, which consist of macro and pico cells. The simulation parameters are set according to a typical two-tier HetNet evaluated in [41], which are summarized in Table II unless otherwise stated. Moreover, the density of UEs is $\lambda_u = 50\lambda_2$ to ensure that the saturation condition is satisfied with high probability.

For Monte Carlo simulation, different realizations of the locations of UEs and BSs are generated according to the PPPs with the respective point densities. For each realization and receiver threshold, the path losses between UEs and their associated BSs are calculated according to the channel model; moreover, by applying FPC with given power control coefficient across the network, the transmit power consumption, achievable data rate, as well as truncation outage events are obtained for evaluating the average energy efficiency. Note that the association results are updated whenever the value of receiver threshold changes. The final results are gathered by averaging over 10^4 realizations.

$$\mathbb{E}[\eta] = \sum_{k=1}^{K} A_k \sum_{n>0} \mathbb{P}(N = n) \int_0^{\infty} \mathbb{P}\{SINR > \tau \,|\, \mathcal{K} = k, N = n\} \, d\eta,$$

$$\mathbb{P}\{SINR > \tau \,|\, \mathcal{K} = k, N = n\}$$

$$= \frac{\delta G_k}{1 - \exp\left(-G_k L_{\max}^{\delta}\right)} \int_0^{L_{max}} l^{\delta-1} \exp\left(-G_k l^{\delta} - \frac{\tau l^{1-\varepsilon}}{SNR} - \frac{\delta L_x^{1-\varepsilon} \tau}{1-\delta} \sum_{j=1}^{K} \left(\frac{P_j}{\sum_{k=1}^{K} P_k}\right)^{1-\delta} A_j G_j\right.$$

$$\left. \times \mathbb{E}_{L_I \leq L_{\max} | \mathcal{K} = k}\left[l_I^{\delta-(1-\varepsilon)} {}_2F_1\left(1, 1-\delta, 2-\delta, -\frac{L_x^{1-\varepsilon} \tau P_j}{l_I^{1-\varepsilon} \sum_{k=1}^{K} P_k}\right)\right]\right) dl \quad (27)$$

$$\mathbb{E}_k[\eta \,|\, K = k] = \int_0^{\infty} \mathbb{P}\left[\frac{W}{N} \cdot \frac{\log 2(1 + SINR)}{P_s + P_{d,t}} > \eta \,|\, K = k\right] d\eta$$

$$= \sum_{n>0} \mathbb{P}[N = n] \int_0^{\infty} \mathbb{P}\left[SINR > 2^{\frac{\eta n(P_s + P_{d,t})}{W}} - 1 \,|\, K = k, N = n\right] d\eta \qquad (29)$$

$$\int_0^{\infty} \mathbb{P}\{SINR > \tau \,|\, \mathcal{K} = k, N = n\} \, d\eta = \int_0^{\infty} \mathbb{P}\left\{\frac{h_{t,o} L_t^{\varepsilon-1}}{SNR^{-1} + \sum_{x \in \Phi_{u\_o}} h_{x,o} L^{\varepsilon}(x, b_x) L_x^{-1}} > \tau \,|\, \mathcal{K} = k, N = n\right\} d\eta$$

$$= \int_0^{\infty} \mathbb{P}\left\{h_{t,o} L_t^{\varepsilon-1} > \tau(SNR^{-1} + \sum_{x \in \Phi_{u\_o}} h_{x,o} L^{\varepsilon}(x, b_x) L_x^{-1}) \,|\, \mathcal{K} = k, N = n\right\} d\eta$$

$$\overset{(a)}{=} \int_0^{\infty} \mathbb{E}\left[\exp\left(-\tau L_x^{1-\varepsilon} SNR^{-1}\right)\right] \cdot \mathcal{L}_{I_r | k_{BS} = k}\left[L_x^{1-\varepsilon} \tau\right] d\eta \qquad (30)$$

$$\mathcal{L}_{I_r | k_{BS} = k}(s) = \exp\left(-\frac{\delta s}{1-\delta} \sum_{j=1}^{K} \left(\frac{P_j}{\sum_{k=1}^{K} P_k}\right)^{1-\delta} A_j G_j \times \mathbb{E}_{L_I \leq L_{\max} | \mathcal{K} = k}\left[l_I^{\delta-(1-\varepsilon)} {}_2F_1\left(1, 1-\delta, 2-\delta, -\frac{s P_j}{l_I^{1-\varepsilon} \sum_{k=1}^{K} P_k}\right)\right]\right)$$

$$(32)$$
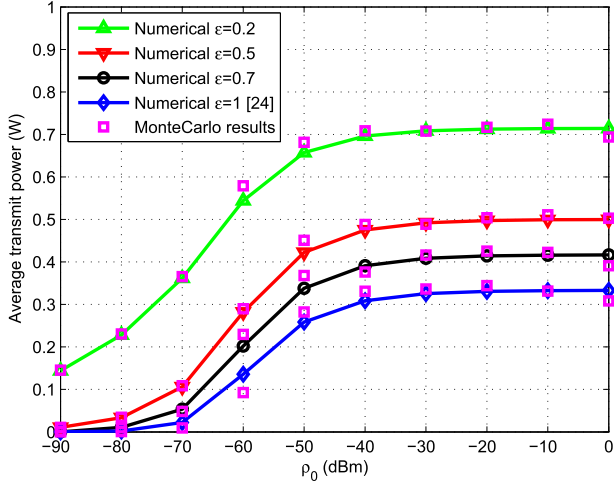
Fig. 4. Average transmit power for different power control coefficients.
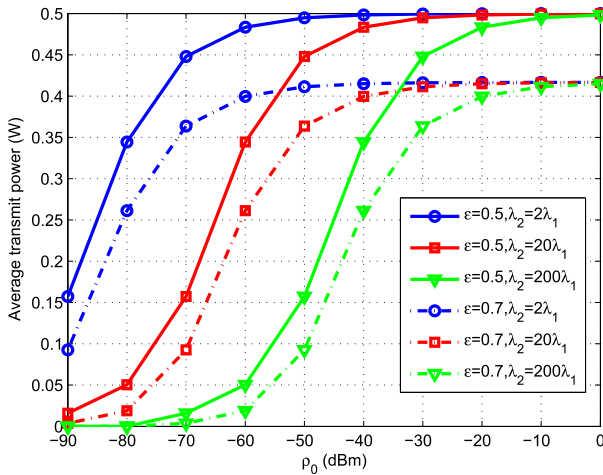
Fig. 5. Average transmit power for different BS densities.

A. Average Transmit Power of UE

Fig. 4 shows the analytical and simulation results for the average transmit power of the uplink UEs under different power control coefficients. We observe that the analytical and simulation results are highly consistent. Meanwhile, the average transmit power increases with the receiver sensitivity ρ_0 for given power control coefficient. Interestingly, the average transmit power increases at a high rate in the low regime of ρ_0, since the uplink UEs require a higher transmit power as the received threshold at their associated BSs increases. However, in the high regime of ρ_0, the average transmit power of uplink UEs saturates due to constrained maximal output power. According to the distance-proportional FPC, the saturation level of average transmit power decreases with power control coefficient for given ρ_0, which is also shown in Fig. 4.

In Fig. 5, we evaluate the average transmit power for different BS densities under $\varepsilon = 0.5$ and $\varepsilon = 0.7$, respectively. As shown in Fig. 5, the average transmit power increases with both the received threshold ρ_0 and the BS density for given ε. Meanwhile, in the high regime of ρ_0, the average transmit power saturates to a constant level whose value is
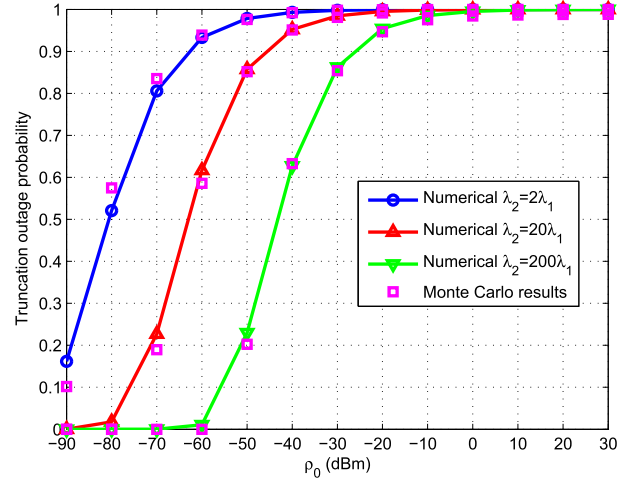
Fig. 6. Truncation outage probability for different BS densities.

independent of BS densities. Similar results have also been observed in [24]. However, we can further show herein that the saturate value is given by $\lim_{\rho_0 \to \infty} \mathbb{E}[P_k] = \frac{\delta}{\delta+\varepsilon} P_{\max}$, based on (24). Recall that when ρ_0 is high, the uplink UEs at cell edges whose required transmit power exceeds $P_{\max}$ will be truncated. Therefore, the average transmit power of active UEs cannot exceed $\frac{\delta}{\delta+\varepsilon} P_{\max}$, which decreases with ε.

B. Truncation Outage Probability of UE

Fig. 6 shows the analytical and simulation results for the truncation outage probability of the two-tier HetNets under different BS densities. We observe that, as expected, the truncation outage probability decreases with the BS densities. In particular, because the average distance between a UE and its associated BS increases as the BS density decreases, the transmit power becomes insufficient to compensate the path loss due to ceiling at the maximal transmit power. Hence, the likelihood of the uplink UE suffering truncation outage is increased while accessing the network. By contrast, for a high BS density, the uplink UE can access the HetNet easily for being close to the BSs. As is consistent with Proposition 3, when receiver threshold ρ_0 is close to maximal output power $P_{\max}$, the truncation outage probability of HetNet will saturate. In this case, large number of UEs will fail in uplink communication, which can deteriorate average uplink energy efficiency in the HetNets.

C. Energy Efficiency of Uplink UEs and Impact of Truncation Outage

1) Average Energy Efficiency Without Truncation Outage: Fig. 7 shows the average uplink energy efficiency for different power control coefficients, where the static power consumption is $P_s = 4$ mW. In Fig. 7, we set the truncation outage probability to be zero. It can be observed that large power control coefficient is always better in this figure. This is because with zero truncation outage probability, UE with small power consumption will achieve a higher uplink energy efficiency. We also find that the average uplink energy efficiency increases with ρ_0 in the low and medium regimes of ρ_0. This is because when ρ_0 is small, UEs with large path loss can still access
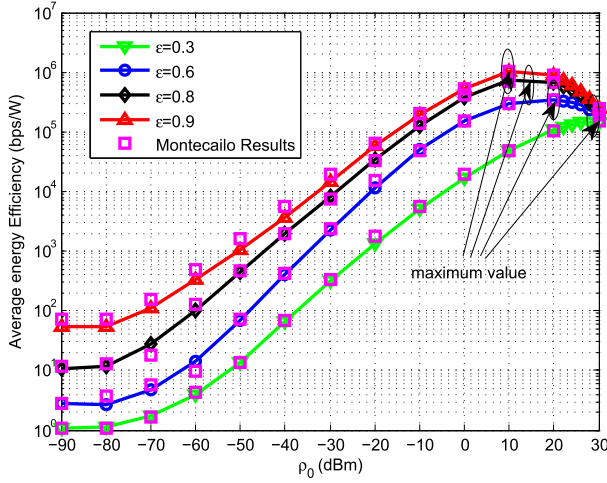
Fig. 7. Average energy efficiency for different power control coefficients without truncation outage.

Fig. 8. Average energy efficiency for different BS densities without truncation outage.

Fig. 9. Effective energy efficiency for different BS densities with truncation outage.

the network, which deteriorates the average energy efficiency. Interestingly, for given ε, there exists an optimal value of average uplink energy efficiency in the high regime of ρ_0. To explain this result, we note that, when ρ_0 is equal to $P_{\max}$, only uplink UEs whose dynamic power consumption is $P_{\max}$ can transmit signals. In this case, the average uplink energy efficiency will converge to the same value $\lim_{\rho_0 \to \infty} \mathbb{E}[\eta] = \frac{R}{P_{\max}+P_s}$ irrespective of the adopted value of ε. On the other hand, when ρ_0 is close to $P_{\max}$, we already know that the average transmit power is $\frac{\delta}{\delta+\varepsilon}P_{\max}$, cf. Fig. 5; in this case, since $\frac{\delta}{\delta+\varepsilon} < 1$, the average uplink energy efficiency can be approximated as $\mathbb{E}[\eta] \approx \frac{R}{\frac{\delta}{\delta+\varepsilon}P_{\max}+P_s}$ and thus decreases with ρ_0 before approaching $P_{\max}$. Therefore, the maximum value of average uplink energy efficiency will appear in the high regime of ρ_0. Moreover, the maximum average uplink energy efficiency increases with power control coefficient since $\frac{\delta}{\delta+\varepsilon}$ decreases with ε. This result also matches our study of the optimal power control coefficient in Fig. 3, where a higher power control coefficient achieves a higher uplink energy efficiency when UEs have a small path loss.

Fig. 8 illustrates the average uplink energy efficiency for different BS densities under $\varepsilon = 0.8$. We observe that the average uplink energy efficiency increases quickly as the BS density λ_2 is increased from $2\lambda_1$ to $20\lambda_1$, while it tends to saturate as λ_2 is increased from $20\lambda_1$ to $200\lambda_1$. The result suggests that we could not enhance the average uplink energy efficiency by only increasing the density of BSs. Interestingly, the optimal receiver threshold for maximizing average uplink energy efficiency decreases with λ_2. This is because, as shown in Fig. 2, the path loss for maximizing uplink energy efficiency decreases with the density of BSs. Note also that, in contrast to Fig. 7, the average uplink energy efficiency curves for different densities of BS in Fig. 8 do not converge as ρ_0 approaches $P_{\max}$. This is because although the saturated average transmit power $\frac{\delta}{\delta+\varepsilon}P_{\max}$ is independent of λ_2, the average load of cell N still depends on the BS density. Nevertheless, the average uplink energy efficiency decreases with ρ_0 with the same slope as ρ_0 approaches $P_{\max}$.
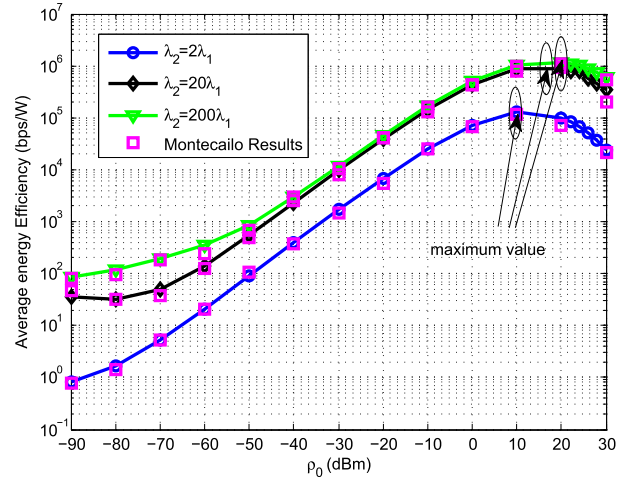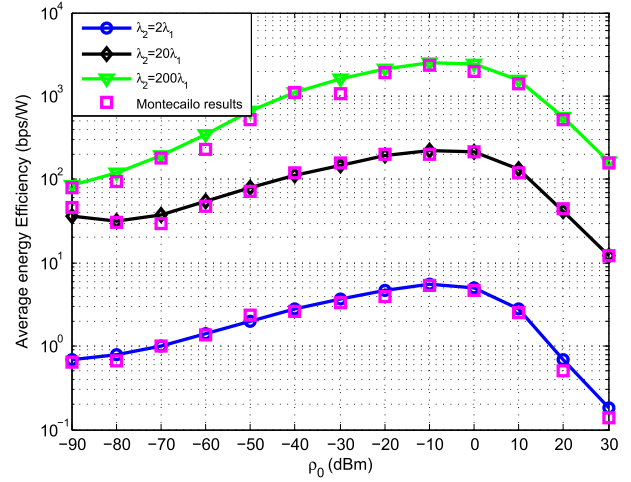
2) Effective Average Energy Efficiency With Truncation Outage: Finally, to show the impact of truncation outage under maximal transmit power constraint, the effective uplink energy efficiency, defined as $(1 - P_{out})\mathbb{E}[\eta]$, is evaluated for different BS densities in Fig. 9. The effective uplink energy efficiency characterizes the average uplink energy efficiency for active UEs. From Fig. 9 we observe that the effective uplink energy efficiency strictly increases with the BS density, since a higher BS density leads to a smaller access distance and thus a lower truncation outage probability. Note that when the density of BSs or the maximal transmit power is large enough, the truncation outage probability becomes small and negligible. In this case, the effective uplink energy efficiency will reduce to average uplink energy efficiency as evaluated in Fig. 7 and Fig. 8. Meanwhile, there exists an optimal receiver threshold for maximization of the effective uplink energy efficiency, implying an interesting trade-off between truncation outage probability and transmission power leveraged by the receiver threshold. In particular, a higher receiver threshold results in a higher truncation outage probability, i.e., more inactive UEs. Therefore, optimal receiver threshold

for maximizing the effective uplink energy efficiency is less than the receiver threshold for maximizing the average uplink energy efficiency.

In fact, Figs. 6–9 also reveal an interesting interplay between truncation outage, power control, and energy efficiency. Recall from Fig. 6 that, when the ρ_0 is larger than 0 dBm, the value of $1 - P_{out}$, i.e., the probability of no truncation outage, is about $10^{-2} \sim 10^{-3}$ for $\lambda_2 = 2\lambda_1$. However, since UEs locate close to their serving BS for $\lambda_2 = 2\lambda_1$, according to Fig. 7, the average EE is as high as 10^6 bps/W by FPC. As a result, the effective uplink EE does not go to zero but reaches about $10^3 \sim 10^4$ bps/W in Fig. 9.

VI. CONCLUSIONS

In this paper, a tractable model was introduced to analyze the energy efficiency of uplink power control in multi-tier HetNet systems. The practical constraint of maximal transmit power at UEs was considered and the impacts of power control coefficient, density of BSs, and receiver threshold on the uplink energy efficiency were investigated. We show the existence of a transfer path loss, by which the access area can be divided into two regions of different properties in terms of energy efficiency. These properties show that the interference from other cells play different roles on the uplink energy efficiency of UEs for different path losses.

The analysis of uplink energy efficiency of UEs was extended to study the average uplink energy efficiency in HetNets. We find that the average transmit power of UEs will be a constant when receiver threshold is high enough. Our results also suggest that the optimal average uplink energy efficiency is obtained when that receiver threshold is close but not equal to the maximal transmit power due to an interesting trade-off between truncation outage and transmission power leveraged by the receiver threshold. Meanwhile, the maximal effective uplink energy efficiency in HetNets can be improved by increasing the density of BS and balancing the values of receiver threshold and power control coefficient.

APPENDIX A
PROOF OF PROPERTY 2

If the path loss l is large enough, the noise can be ignored and the uplink energy efficiency $\eta(l, \varepsilon)$ can be expanded

through Taylor's theorem for $l > l^*$ as (A.1), shown at the bottom of the this page.

Then $\left| \eta(l, \varepsilon) - N(l) / D(\varepsilon) \right| \leqslant N(l) P_u^{-1}(\varepsilon) I^{-2}(\varepsilon) h_{t,o} l^{\varepsilon-1}$.

For $\varepsilon \in [0, 1]$, $\varepsilon - 1 \leqslant 0$, such that both $N(l)$ and $l^{\varepsilon-1}$ are mono-decreasing function for $l > l^*$. The gap between $\eta(l, \varepsilon)$ and $N(l) / D(\varepsilon)$ will be close to zero as the path loss of UE increasing. We can get $N(l) P_u^{-1}(\varepsilon) I^{-2}(\varepsilon) h_{t,o} l^{\varepsilon-1} \leqslant N(l^*) P_u^{-1}(\varepsilon) I^{-2}(\varepsilon) h_{t,o} l^{*(\varepsilon-1)}$, where the equality holds with $\varepsilon = 1$.

APPENDIX B
PROOF OF PROPERTY 3

In the region of $l < l^*$, we have (B.1), shown at the bottom of this page. Since $\varepsilon - 1 < 0$, it is easy to verify that $\frac{\partial \eta(l, \varepsilon)}{\partial l} < 0$, i.e., $\eta(l, \varepsilon)$ is decreasing with l.

According to $\frac{ax}{1+ax} < \ln(1 + ax)$ for $x > -1$, we get

$$\ln\left(1 + h_{t,o} l^{(\varepsilon-1)} I^{-1}(\varepsilon)\right) > \frac{h_{t,o} l^{(\varepsilon-1)} I^{-1}(\varepsilon)}{1 + h_{t,o} l^{(\varepsilon-1)} I^{-1}(\varepsilon)}. \quad \text{(B.2)}$$

Substituting (B.2) into (B.1), we obtain the inequalities in (B.3), shown at the top of the next page. Therefore, we have

$$-\frac{\log_2 e}{P_u(\varepsilon) l^{\varepsilon+1}} \ln\left(1 + h_{t,o} l^{(\varepsilon-1)} I^{-1}(\varepsilon)\right) < \frac{\partial \eta(l, \varepsilon)}{\partial l}$$

$$< -\frac{\log_2 e}{P_u(\varepsilon) l^{\varepsilon+1}} \frac{h_{t,o} l^{(\varepsilon-1)} I^{-1}(\varepsilon)}{1 + h_{t,o} l^{(\varepsilon-1)} I^{-1}(\varepsilon)}. \quad \text{(B.4)}$$

Since both $l^{(\varepsilon-1)}$ and $I^{-1}(\varepsilon)$ are decreasing with ε, such that $\ln\left(1 + h_{t,o} l^{(\varepsilon-1)} I^{-1}(\varepsilon)\right)$ and $\frac{h_{t,o} l^{(\varepsilon-1)} I^{-1}(\varepsilon)}{1 + h_{t,o} l^{(\varepsilon-1)} I^{-1}(\varepsilon)}$ is decreasing with ε. Meanwhile, $l^{-(\varepsilon+1)}$ are decreasing with ε, such that both left and right hand sides of (B.4) increase with ε. Then according to the Squeeze Theorem, $\frac{\partial \eta(l, \varepsilon)}{\partial l}$ is mono-increasing with ε.

APPENDIX C
PROOF OF THEOREM 2

For given path loss l, there always exists a power control coefficient $\varepsilon \neq 1$, such that the uplink energy efficiency satisfies $\eta_s(\varepsilon, l) > \eta_s(1, l)$, or equivalently,

$$\frac{\log_2\left(1 + h_{t,o} l^{(\varepsilon-1)} I^{-1}(\varepsilon)\right)}{P_u(\varepsilon) l^\varepsilon} > \frac{\log_2\left(1 + h_{t,o} I^{-1}(1)\right)}{P_u(\varepsilon) l}. \quad \text{(C.1)}$$

$$\begin{aligned}
\frac{\eta(l, \varepsilon)}{N(l) / D(\varepsilon)} &= \frac{B \log_2\left(1 + h_{t,o} l^{(\varepsilon-1)} I^{-1}(\varepsilon)\right)}{P_u(\varepsilon) l^\varepsilon} \frac{D(\varepsilon)}{N(l)} \\
&= \frac{\left(h_{t,o} l^{(\varepsilon-1)} I^{-1}(\varepsilon) + \frac{\left(h_{t,o} l^{(\varepsilon-1)} I^{-1}(\varepsilon)\right)^2}{2!} + O\left(\left(h_{t,o} l^{(\varepsilon-1)} I^{-1}(\varepsilon)\right)^2\right)\right)}{h_{t,o} l^{(\varepsilon-1)} I^{-1}(\varepsilon)} \\
&\leq \left(1 + h_{t,o} l^{(\varepsilon-1)} I^{-1}(\varepsilon)\right)
\end{aligned} \quad \text{(A.1)}$$

$$\frac{\partial \eta(l, \varepsilon)}{\partial l} = \frac{\log_2 e}{P_u(\varepsilon) l^{2\varepsilon}} \left(\frac{(\varepsilon - 1) h_{t,o} l^{(2\varepsilon-2)} I^{-1}(\varepsilon)}{1 + h_{t,o} l^{(\varepsilon-1)} I^{-1}(\varepsilon)} - \varepsilon \ln\left(1 + h_{t,o} l^{(\varepsilon-1)} I^{-1}(\varepsilon)\right) l^{(\varepsilon-1)}\right) \quad \text{(B.1)}$$

$$\frac{\log_2 e}{P_u(\varepsilon) l^{\varepsilon+1}} \left((\varepsilon-1) \ln\left(1 + h_{t,o} l^{(\varepsilon-1)} I^{-1}(\varepsilon)\right) - \varepsilon \ln\left(1 + h_{t,o} l^{(\varepsilon-1)} I^{-1}(\varepsilon)\right)\right)$$

$$< \frac{\partial \eta(l,\varepsilon)}{\partial l} < \frac{\log_2 e}{P_u(\varepsilon) l^{\varepsilon+1}} \left(\frac{(\varepsilon-1) h_{t,o} l^{(\varepsilon-1)} I^{-1}(\varepsilon)}{1 + h_{t,o} l^{(\varepsilon-1)} I^{-1}(\varepsilon)} - \frac{\varepsilon h_{t,o} l^{(\varepsilon-1)} I^{-1}(\varepsilon)}{1 + h_{t,o} l^{(\varepsilon-1)} I^{-1}(\varepsilon)} \right) \tag{B.3}$$

By simplifying (C.1), we get

$$l^{1-\varepsilon} \ln\left(1 + h_{t,o} l^{(\varepsilon-1)} I^{-1}(\varepsilon)\right) > \ln\left(1 + h_{t,o} I^{-1}(1)\right). \tag{C.2}$$

Since inequality $\frac{ax}{1+ax} < \ln(1+ax) < ax$ holds for $ax > -1$ and $x \neq 0$, we have

$$l^{1-\varepsilon} \ln\left(1 + h_{t,o} l^{(\varepsilon-1)} I^{-1}(\varepsilon)\right) > \frac{h_{t,o} I^{-1}(\varepsilon)}{1 + h_{t,o} l^{(\varepsilon-1)} I^{-1}(\varepsilon)}. \tag{C.3}$$

Substituting (C.3) into (C.2), we have $\frac{h_{t,o} I^{-1}(\varepsilon)}{1 + h_{t,o} l^{(\varepsilon-1)} I^{-1}(\varepsilon)} > \ln\left(1 + h_{t,o} I^{-1}(1)\right)$, whose solution is

$$l > \left(\frac{1}{\ln\left(1 + h_{t,o} I^{-1}(1)\right)} - \frac{1}{h_{t,o} I^{-1}(\varepsilon)} \right)^{\frac{1}{\varepsilon-1}}. \tag{C.4}$$

Therefore, for any $\varepsilon \in (0,1)$, path loss should be smaller than $\lim_{\varepsilon \to 1} \left(\frac{1}{\ln(1+h_{t,o} I^{-1}(1))} - \frac{1}{h_{t,o} I^{-1}(\varepsilon)} \right)^{\frac{1}{\varepsilon-1}} = \exp\left(\left(\frac{h_{t,o} I(1)}{\ln(1+h_{t,o} I(1))} - 1 \right)^{-1} \cdot \frac{I'(1)}{I(1)} \right)$ such that complete channel inversion power control $\eta(1,l)$ have better uplink energy efficiency than $\eta(\varepsilon, l)$.

If constant power control ($\varepsilon = 0$) have better energy efficiency than any other ε, that is

$$\frac{\log_2\left(1 + h_{t,o} l^{(\varepsilon-1)} I^{-1}(\varepsilon)\right)}{P_u(\varepsilon) l^{\varepsilon}} < \frac{\log_2\left(1 + h_{t,o} I^{-1}(0)\right)}{P_u(\varepsilon)}. \tag{C.5}$$

(C.5) can be rewritten as

$$l^{-\varepsilon} \ln\left(1 + h_{t,o} l^{(\varepsilon-1)} I^{-1}(\varepsilon)\right) < \ln\left(1 + h_{t,o} I^{-1}(0)\right). \tag{C.6}$$

According to inequality $\frac{ax}{1+ax} < \ln(1+ax) < ax$, we obtain

$$l^{-\varepsilon} \ln\left(1 + h_{t,o} l^{(\varepsilon-1)} I^{-1}(\varepsilon)\right) < h_{t,o} l^{-1} I^{-1}(\varepsilon). \tag{C.7}$$

That is if $\ln\left(1 + h_{t,o} I^{-1}(0)\right) > h_{t,o} l^{-1} I^{-1}(\varepsilon)$, i.e. $l > \frac{h_{t,o} I^{-1}(\varepsilon)}{\ln(1+h_{t,o} I^{-1}(0))}$, constant power control ($\varepsilon = 0$) have better energy efficiency than $\eta(\varepsilon, l)$.

According to Property 3, the path loss l is decreasing for optimal power control coefficient ε^*. We can obtain that when $l > \frac{h_{t,o} I^{-1}(0)}{\ln(1+h_{t,o} I^{-1}(0))}$, constant power control ($\varepsilon = 0$) have the highest uplink energy efficiency for any ε and when $l < \exp\left(\left(\frac{h_{t,o} I(1)}{\ln(1+h_{t,o} I(1))} - 1 \right)^{-1} \cdot \frac{I'(1)}{I(1)} \right)$, complete channel inversion power control ($\varepsilon = 1$) have the highest uplink energy efficiency for any ε.

REFERENCES

[1] Cisco, "Cisco visual networking index: Global mobile data traffic forecast update 2015–2020," White Paper, Feb. 2016.

[2] H. A. Ul Mustafa, M. A. Imran, M. Z. Shakir, A. Imran, and R. Tafazolli, "Separation framework: An enabler for cooperative and D2D communication for future 5G networks," *IEEE Commun. Surveys Tuts.*, vol. 18, no. 1, pp. 419–445, 1st Quart., 2016.

[3] D. Tse and P. Viswanath, *Fundamentals Wireless Communication*. Cambridge, U.K.: Cambridge Univ. Press, 2005.

[4] G. Miao *et al.*, "Cross-layer optimization for energy-efficient wireless communications: A survey," *J. Wireless Commun. Mobile Comput.*, vol. 9, no. 4, pp. 529–542, Apr. 2009.

[5] G. Auer *et al.*, "How much energy is needed to run a wireless network?" *IEEE Wireless. Commun.*, vol. 18, no. 5, pp. 40–49, Oct. 2011.

[6] G. Y. Li *et al.*, "Energy-efficient wireless communications: Tutorial, survey, and open issues," *IEEE Wireless. Commun.*, vol. 18, no. 6, pp. 28–35, Dec. 2011.

[7] Y. Chen *et al.*, "Fundamental trade-offs on green wireless networks," *IEEE Commun. Mag.*, vol. 49, no. 6, pp. 30–37, Jun. 2011.

[8] X. Li, X. Ge, X. Wang, J. Cheng, and V. C. M. Leung, "Energy efficiency optimization: Joint antenna-subcarrier-power allocation in OFDM-DASs," *IEEE Trans. Wireless Commun.*, vol. 15, no. 11, pp. 7470–7483, Nov. 2016.

[9] Q. Wu, W. Chen, M. Tao, J. Li, H. Tang, and J. Wu, "Resource allocation for joint transmitter and receiver energy efficiency maximization in downlink OFDMA systems," *IEEE Trans. Commun.*, vol. 63, no. 2, pp. 416–430, Feb. 2015.

[10] F. Richter, A. J. Fehske, and G. P. Fettweis, "Energy efficiency aspects of base station deployment strategies for cellular networks," in *Proc. IEEE VTC-Fall.*, Sep. 2009, pp. 1–5.

[11] P.-S. Yu, J. Lee, T. Q. S. Quek, and Y.-W. P. Hong, "Traffic offloading in heterogeneous networks with energy harvesting personal cells-network throughput and energy efficiency," *IEEE Trans. Wireless Commun.*, vol. 15, no. 2, pp. 1146–1161, Feb. 2016.

[12] Q. Wu, G. Y. Li, W. Chen, and D. W. K. Ng, "Energy-efficient small cell with spectrum-power trading," *IEEE J. Sel. Areas Commun.*, vol. 34, no. 12, pp. 3394–3408, Dec. 2016.

[13] *Uplink Power Control for E-UTRA-Range and Representation of P0*, document 3GPP TSG RAN WG1, R1-074850, Ericsson, Stockholm, Sweden, Nov. 2007

[14] R. Müllner, C. F. Ball, K. Ivanov, J. Lienhart, and P. Hric, "Contrasting open-loop and closed-loop power control performance in UTRAN LTE uplink by UE trace analysis," in *Proc. IEEE Int. Conf. Commun. (ICC)*, Jun. 2009, pp. 1–6.

[15] B. Muhammad and A. Mohammed, "Performance evaluation of uplink closed loop power control for LTE system," in *Proc. IEEE VTC-Fall*, Sep. 2009, pp. 1–5.

[16] C. Castellanos *et al.*, "Performance of uplink fractional power control in UTRAN LTE," in *Proc. IEEE VTC*, May 2008, pp. 2517–2521.

[17] M. Coupechoux and J.-M. Kelif, "How to set the fractional power control compensation factor in LTE?" in *Proc. IEEE Sarnoff Symp.*, May 2011, pp. 1–5.

[18] H. Elsawy, E. Hossain, and M. Haenggi, "Stochastic geometry for modeling, analysis, and design of multi-tier and cognitive cellular wireless networks: A survey," *IEEE Commun. Surveys Tuts.*, vol. 15, no. 3, pp. 996–1019, 3rd Quart., 2013.

[19] J. G. Andrews, F. Baccelli, and R. K. Ganti, "A tractable approach to coverage and rate in cellular networks," *IEEE Trans. Commun.*, vol. 59, no. 11, pp. 3122–3134, Nov. 2011.

[20] J. Xu, J. Zhang, and J. G. Andrews, "On the accuracy of the Wyner model in cellular networks," *IEEE Trans. Wireless Commun.*, vol. 10, no. 9, pp. 3098–3109, Sep. 2011.

[21] H. S. Dhillon and J. G. Andrews, "Downlink rate distribution in heterogeneous cellular networks under generalized cell selection," *IEEE Wireless Commun. Lett.*, vol. 3, no. 1, pp. 42–45, Feb. 2014.

[22] M. Haenggi, *Stochastic Geometry for Wireless Networks*, Cambridge, U.K.: Cambridge Univ. Press, 2012.

[23] T. D. Novlan, H. S. Dhillon, and J. G. Andrews, "Analytical modeling of uplink cellular networks," *IEEE Trans. Wireless Commun.*, vol. 12, no. 6, pp. 2669–2679, Jun. 2013.

[24] H. ElSawy and E. Hossain, "On stochastic geometry modeling of cellular uplink transmission with truncated channel inversion power control," *IEEE Trans. Wireless Commun.*, vol. 13, no. 8, pp. 4454–4469, Aug. 2014.

[25] J. B. Rao and A. O. Fapojuwo, "Analysis of spectrum efficiency and energy efficiency of heterogeneous wireless networks with intra-/inter-RAT offloading," *IEEE Trans. Veh. Technol.*, vol. 64, no. 7, pp. 3120–3139, Jul. 2015.

[26] J. B. Rao and A. O. Fapojuwo, "An analytical framework for evaluating spectrum/energy efficiency of heterogeneous cellular networks," *IEEE Trans. Veh. Technol.*, vol. 65, no. 5, pp. 3568–3584, May 2016.

[27] K. Davaslioglu, C. C. Coskun, and E. Ayanoglu, "Energy-efficient resource allocation for fractional frequency reuse in heterogeneous networks," *IEEE Trans. Wireless Commun.*, vol. 14, no. 10, pp. 5484–5497, Oct. 2015.

[28] E Chavarria-Reyes, I. F. Akyildiz, and E. Fadel, "Energy-efficient multi-stream carrier aggregation for heterogeneous networks in 5G wireless systems," *IEEE Trans. Wireless Commun.*, vol. 15, no. 11, pp. 7432–7443, Nov. 2016.

[29] S. Singh, X. Zhang, and J. G. Andrews, "Joint rate and SINR coverage analysis for decoupled uplink-downlink biased cell associations in HetNets," *IEEE Trans. Wireless Commun.*, vol. 14, no. 10, pp. 5360–5373, Oct. 2015.

[30] B. Blaszczyszyn, M. K. Karray, and H. P. Keeler, "Using Poisson processes to model lattice cellular networks," in *Proc. IEEE INFOCOM*, Apr. 2013, pp. 773–781.

[31] M. Haenggi, "User point processes in cellular networks," *IEEE Wireless Commun. Lett.*, vol. 6, no. 2, pp. 258–261, Apr. 2017.

[32] N. Jindal, S. Weber, and J. G. Andrews, "Fractional power control for decentralized wireless networks," *IEEE Trans. Wireless Commun.*, vol. 7, no. 12, pp. 5482–5492, Dec. 2008.

[33] H.-S. Jo, Y. J. Sang, P. Xia, and J. G. Andrews, "Heterogeneous cellular networks with flexible cell association: A comprehensive downlink SINR analysis," *IEEE Trans. Wireless Commun.*, vol. 11, no. 10, pp. 3484–3495, Oct. 2012.

[34] R. Ruby, V. C. M. Leung, and D. G. Michelson, "Uplink scheduler for SC-FDMA-based heterogeneous traffic networks with QoS assurance and guaranteed resource utilization," *IEEE Trans. Veh. Technol.*, vol. 64, no. 10, pp. 4780–4796, Oct. 2015.

[35] B. Błaszczyszyn and D. Yogeshwaran, "Clustering comparison of point processes, with applications to random geometric models," in *Stochastic Geometry, Spatial Statistics and Random Fields* (Lecture Notes in Mathematics), vol. 2120. Cham, Switzerland: Springer-Verlag, 2015, pp. 31–71.

[36] S. Singh, F. Baccelli, and J. G. Andrews, "On association cells in random heterogeneous networks," *IEEE Wireless Commun. Lett.*, vol. 3, no. 1, pp. 70–73, Feb. 2014.

[37] G. H. Hardy, J. E. Littlewood, and G. Polya, *Inequalities*, 2nd ed. Cambridge, U.K.: Cambridge Univ. Press, 1988.

[38] J. Pečarić, F. Qi, V. Šimić, and S.-L. Xu, "Refinements and extensions of an inequality, III," *J. Math. Anal. Appl.*, vol. 227, no. 2, pp. 439–448, Nov. 1998.

[39] D. W. K. Ng, E. S. Lo, and R. Schober, "Energy-efficient resource allocation in multi-cell OFDMA systems with limited backhaul capacity," *IEEE Trans. Wireless Commun.*, vol. 11, no. 10, pp. 3618–3631, Oct. 2012.

[40] I. S. Gradshteyn and I. M. Ryzhik, *Table of Integrals, Series, and Products*, 5th ed. New York, NY, USA: Academic, 2007.

[41] S. Singh, H. S. Dhillon, and J. G. Andrews, "Offloading in heterogeneous networks: Modeling, analysis, and design insights," *IEEE Trans. Wireless Commun.*, vol. 12, no. 5, pp. 2484–2497, May 2013.

[42] Y. Chen, Y. Wang, R. Zhang, and X. Shen, "Optimization on power splitting ratio design for K-tier HCNs with opportunistic energy harvesting," in *Proc. IEEE Int. Conf. Commun. (ICC)*, Jun. 2015, pp. 1500–1505.

Jing Zhang (M'13) received the M.S. and Ph.D. degrees in electronics and information engineering from the Huazhong University of Science and Technology (HUST), Wuhan, China, in 2002 and 2010, respectively. He is currently an Associate Professor with HUST. He has done research in the areas of multiple-input multiple-output, CoMP, beamforming, and next-generation mobile communications. His current research interests include HetNet in 5G, green communications, energy harvesting, Internet of Things, optimization, and performance analysis in networks. He received the Best Paper Award at the IEEE Globecom Communication Workshop in 2014 and the International Wireless Communications and Mobile Computing Conference in 2015.

Lin Xiang (S'14) received the bachelor's and master's degrees from the Department of Electronics and Information Engineering, Huazhong University of Science and Technology, China, in 2009 and 2012, respectively. He is currently pursuing the Ph.D. degree with the Institute for Digital Communication, Friedrich-Alexander University of Erlangen-Nuremberg, Germany. From 2010 to 2011, he was an exchange student with the University of Bologna, Italy, under support from the Erasmus Mundus Programme. His research interests include modeling and analysis of traffic load and energy efficiency in wireless networks, performance analysis based on stochastic geometry theory, renewable energy integration and electric vehicle charging in smart grid, and resource allocation for cache-aided wireless communication systems. He received the Best Paper Award at the IEEE Globecom Communication Conference in 2010.

Derrick Wing Kwan Ng (S'06–M'12) received the bachelor's degree (Hons.) and the M.Phil. degree in electronic engineering from The Hong Kong University of Science and Technology in 2006 and 2008, respectively, and the Ph.D. degree from The University of British Columbia in 2012. In 2011 and 2012, he was a Visiting Scholar with the Centre Tecnològic de Telecomunicacions de Catalunya, Hong Kong. He was a Senior Post-Doctoral Fellow with the Institute for Digital Communications, Friedrich-Alexander-University Erlangen-Nürnberg, Germany. He is currently a Senior Lecturer and an ARC DECRA Research Fellow with the University of New South Wales, Sydney, Australia. His research interests include convex and non-convex optimization, physical layer security, wireless information and power transfer, and green (energy-efficient) wireless communications. He received Best Paper Awards at the IEEE International Conference on Computing, Networking and Communications in 2016, the IEEE Wireless Communications and Networking Conference in 2012, the IEEE Global Telecommunication Conference in 2011, and the IEEE Third International Conference on Communications and Networking in China in 2008. He has been serving as an Editorial Assistant to the Editor-in-Chief of the IEEE TRANSACTIONS ON COMMUNICATIONS since 2012. He is currently an Editor of the IEEE COMMUNICATIONS LETTERS, the IEEE TRANSACTIONS ON WIRELESS COMMUNICATIONS, and the IEEE TRANSACTIONS ON GREEN COMMUNICATIONS AND NETWORKING.

Minho Jo (M'07–SM'16) received the B.A. degree from the Department of Industrial Engineering, Chosun University, South Korea, in 1984, and the Ph.D. degree from the Department of Industrial and Systems Engineering, Lehigh University, Bethlehem, PA, USA, in 1994. He was the Founder of the ICT Team, LCD Division, Samsung Electronics, in 1995. He is currently a Professor with the Department of Computer Convergence Software, Korea University, Sejong Metropolitan City, South Korea. He is also the Chief Professor of IoTCoN Lab, Korea University. He is one of founders of the Samsung Electronics LCD Division. His current interests include LTE-U, cognitive radio, IoT, machine learning in IoT, HetNets in 5G, energy-efficient wireless communications, cloud computing, big data in IoT, network function virtualization, 5G wireless communications, optimization and probability in networks, network security, and massive MIMO. He received the Headong Outstanding Scholar Prize in 2011. He was the Vice President of the Institute of Electronics and Information Engineers and the Korea Information Processing Society. He is currently the Founding Vice President of 4th Industrial Revolution Society and the Vice President of the Korean Society for Internet Information. He is the Founder and an Editor-in-Chief of the KSII *Transactions on Internet and Information Systems* (SCI and SCOPUS indexed, respectively). He is currently an Editor of the IEEE WIRELESS COMMUNICATIONS and an Associate Editor of the IEEE INTERNET OF THINGS JOURNAL, *Security and Communication Networks*, and WIRELESS COMMUNICATIONS AND MOBILE COMPUTING.

Min Chen (SM'09) was an Assistant Professor with the School of Computer Science and Engineering, Seoul National University (SNU). He was a Post-Doctoral Fellow with SNU for one and half years. He was a Post-Doctoral Fellow with the Department of Electrical and Computer Engineering, The University of British Columbia for three years. He has been a Full Professor with the School of Computer Science and Technology, Huazhong University of Science and Technology (HUST), since 2012. He is currently the Director of the Embedded and Pervasive Computing Lab, HUST. He has over 300 paper publications, including over 200 SCI papers, over 80 IEEE transactions/journal papers, 13 ISI highly cited papers, and eight hot papers. He has published four books: *OPNET IoT Simulation* (HUST Press, 2015), *Big Data Inspiration* (HUST Press, 2015), *5G Software Defined Networks* (HUST Press, 2016), and *Introduction to Cognitive Computing* (HUST Press, 2017), a book on big data: *Big Data Related Technologies* (Springer Series, 2014) and a book on 5G: *Cloud Based 5G Wireless Networks* (Springer Series, 2016) in computer science. His latest book, co-authored with Prof. K. Hwang, is *Big Data Analytics for Cloud/IoT and Cognitive Computing* (Wiley, U.K., 2017). His research focuses on cyber physical systems, IoT sensing, 5G networks, mobile cloud computing, SDN, healthcare big data, medica cloud privacy and security, body area networks, emotion communications, and robotics. He received the Best Paper Award from QShine 2008, the IEEE ICC 2012, ICST IndustrialIoT 2016, and the IEEE IWCMC 2016. He received the IEEE Communications Society Fred W. Ellersick Prize in 2017. He is the Chair of the IEEE Computer Society Special Technical Communities on Big Data. He is a Co-Chair of the IEEE ICC 2012 Communications Theory Symposium and a Co-Chair of the IEEE ICC 2013 Wireless Networks Symposium. He is a General Co-Chair for the IEEE CIT-2012, Tridentcom 2014, Mobimedia 2015, and Tridentcom 2017. He was a Keynote Speaker at CyberC 2012, Mobiquitous 2012, Cloudcomp 2015, IndustrialIoT 2016, and the 7th Brainstorming Workshop on 5G Wireless. He serves as an Editor or an Associate Editor of *Information Sciences*, *Information Fusion*, and IEEE ACCESS. He is a Guest Editor of the IEEE NETWORK, the IEEE WIRELESS COMMUNICATIONS, and the IEEE TRANSACTIONS ON SERVICE COMPUTING. His Google Scholars Citations reached over 9,700 with an h-index of 49. His top paper was cited over 1000 times.